To appear as a part of an upcoming textbook on dimensionality reduction and manifold learning.

Unified Framework for Spectral Dimensionality Reduction, Maximum Variance Unfolding, and Kernel Learning By Semidefinite Programming: Tutorial and Survey

Benyamin Ghojogh   BGHOJOGH@UWATERLOO.CA
Department of Electrical and Computer Engineering,
Machine Learning Laboratory, University of Waterloo, Waterloo, ON, Canada

Ali Ghodsi   ALI.GHODSI@UWATERLOO.CA
Department of Statistics and Actuarial Science & David R. Cheriton School of Computer Science,
Data Analytics Laboratory, University of Waterloo, Waterloo, ON, Canada

Fakhri Karray   KARRAY@UWATERLOO.CA
Department of Electrical and Computer Engineering,
Centre for Pattern Analysis and Machine Intelligence, University of Waterloo, Waterloo, ON, Canada

Mark Crowley   MCROWLEY@UWATERLOO.CA
Department of Electrical and Computer Engineering,
Machine Learning Laboratory, University of Waterloo, Waterloo, ON, Canada

Abstract

This is a tutorial and survey paper on unification of spectral dimensionality reduction methods, kernel learning by Semidefinite Programming (SDP), Maximum Variance Unfolding (MVU) or Semidefinite Embedding (SDE), and its variants. We first explain how the spectral dimensionality reduction methods can be unified as kernel Principal Component Analysis (PCA) with different kernels. This unification can be interpreted as eigenfunction learning or representation of kernel in terms of distance matrix. Then, since the spectral methods are unified as kernel PCA, we say let us learn the best kernel for unfolding the manifold of data to its maximum variance. We first briefly introduce kernel learning by SDP for the transduction task. Then, we explain MVU in detail. Various versions of supervised MVU using nearest neighbors graph, by class-wise unfolding, by Fisher criterion, and by colored MVU are explained. We also explain out-of-sample extension of MVU using eigenfunctions and kernel mapping. Finally, we introduce other variants of MVU including action respecting embedding, re-

laxed MVU, and landmark MVU for big data.

1. Introduction

Dimensionality reduction algorithms can be divided into three categories which are spectral, probabilistic, and neural network-based methods (Ghojogh, 2021). Spectral dimensionality reduction methods deal with geometry of data and sometimes reduce to an eigenvalue or generalized eigenvalue problem (Ghojogh et al., 2019a). Various spectral methods have been proposed during decades. Some of the most well-known spectral methods are Principal Component Analysis (PCA) (Ghojogh & Crowley, 2019), Multidimensional Scaling (MDS), Isomap (Ghojogh et al., 2020b), spectral clustering, Laplacian eigenmap, diffusion map (Ghojogh et al., 2021a), and Locally Linear Embedding (LLE) (Ghojogh et al., 2020a). After development of many of these methods, it was found out that the spectral methods are all learning eigenfunctions and can be reduced to kernel PCA with different kernels (Bengio et al., 2003b;c;a; 2004; 2006). Moreover, from the formulation of MDS, we know that we can write kernel in terms of the distance matrix (Ghojogh et al., 2020b). It was shown in (Ham et al., 2004) that the spectral methods can be seen as kernel PCA with different kernels where kernels are constructed from various distance matrices. Hence, the spectral methods can be unified as kernel PCA theoretically. This kernel-based unified framework for the spectral dimensionality re-
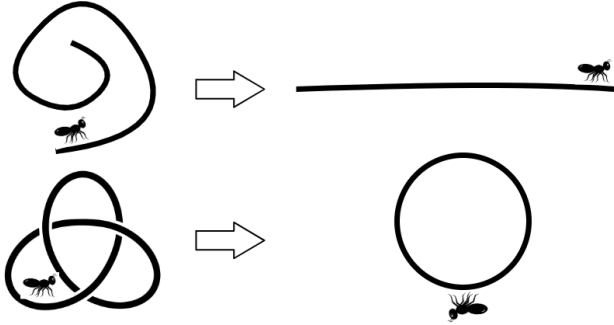
Figure 1. The intrinsic dimensionality for Swiss roll (above) and trefoil knot (below). Suppose a small ant, which cannot see the whole manifold together and can only see its front, traverses the manifold once completely. The dimensionality that the ant feels by this traversing is the intrinsic dimensionality. For example, the intrinsic dimensionalities of 2D Swiss roll and 3D trefoil knot are one and two, respectively, because the ant reaches an end of line in the former (so it is like a 1D line) and the ant reaches to its starting point in the latter (so it is like a 2D circle).

duction encouraged the researchers to obtain the best kernel matrix for every specific dataset.

Around the time of discovery of this unification, it was found out in (Lanckriet et al., 2004) that the kernel matrix can be learned using Semidefinite Programming (SDP) (Vandenberghe & Boyd, 1996). This kernel learning was proposed for the goal of transduction, i.e., learning the labels of an unlabeled part of data. The fact that the kernel can be learned by SDP inspired researchers to use SDP for learning the best kernel for dimensionality reduction and manifold unfolding. They said now that we knew the spectral methods can be seen as kernel PCA with different kernels, let us learn the best kernel for manifold unfolding to its maximum variance. Hence, Semidefinite Embedding (SDE) (Weinberger et al., 2004; Weinberger & Saul, 2004; Weinberger et al., 2005; Weinberger & Saul, 2006b) was proposed which was later renamed to Maximum Variance Unfolding (MVU) (Weinberger & Saul, 2006a). MVU unfolds manifold to its maximum variance in its intrinsic dimensionality. For understanding the intuition of intrinsic dimensionality, see Fig. 1. The task of manifold unfolding to its maximum variance is depicted by an example in Fig. 2. After proposal of MVU, various versions of MVU were developed such as supervised MVU (Zhang et al., 2005; Liu et al., 2005; Song et al., 2007; Wei et al., 2016), landmark MVU (Weinberger et al., 2005), action respecting embedding (Bowling et al., 2005), out-of-sample extensions (Chin & Suter, 2008), relaxed MVU (Hou et al., 2008), etc.

The remainder of this paper is organized as follows. We explain unification of spectral dimensionality reduction methods as kernel PCA in Section 2. Required background on SDP is introduced in Section 3. We introduce kernel learning by SDP for the transduction task in Section 4. MVU or SDE is explained in detail in Section 5. We explain supervised MVU using nearest neighbors graph, by class-wise unfolding, by Fisher criterion, and by colored MVU in Section 6. Out-of-sample extensions of MVU using eigenfunctions and kernel mapping are explained in Section 7. Some other variants of MVU including action respecting embedding, relaxed MVU, and landmark MVU for big data are introduced in Section 8. Finally, Section 9 concludes the paper.

Required Background for the Reader

This paper assumes that the reader has general knowledge of calculus, linear algebra, and basics of optimization.

2. Unified Framework for Spectral Methods

After development of many spectral dimensionality reduction methods, it was found out by researchers that these methods all can be unified as kernel Principal Component Analysis (PCA) (Ghojogh & Crowley, 2019) with different kernels. This is mostly because the spectral methods reduce to an eigenvalue or a generalized eigenvalue problem (Ghojogh et al., 2019a). This unification can be analyzed from different perspectives including eigenfunction learning, having kernels in kernel PCA, and generalized embedding. In the following, we explain these points of view.

2.1. Learning Eigenfunctions

After some initial work was done in (Williams & Seeger, 2000) on using eigenfunctions in machine learning, Bengio et. al. developed eigenfunctions learning and showed that the spectral methods actually learn eigenfunctions (Bengio et al., 2003b;c;a; 2004; 2006). In the following, we repeat some contents from our other tutorial (Ghojogh et al., 2021b) for the sake of explanation. Refer to (Ghojogh et al., 2021b) for more details and proofs about eigenfunctions and embedding using eigenfunctions.

First, consider The eigenvalue problem for the kernel matrix (Ghojogh et al., 2019a):

$$\boldsymbol{K}\boldsymbol{v}_k = \delta_k \boldsymbol{v}_k, \quad \forall k \in \{1, \ldots, n\}, \qquad (1)$$

where $\boldsymbol{v}_k$ is the k-th eigenvector and δ_k is the corresponding eigenvalue.

Definition 1 (Eigenfunction (Ghojogh et al., 2021b)). *Consider a linear operator O which can be applied on a function f. If applying this operator on the function results in a multiplication of function to a constant:*

$$Of = \lambda f, \qquad (2)$$

then the function f is an eigenfunction for the operator O and the constant λ is the corresponding eigenvalue.

Figure 2. Iterative unfolding of a nonlinear Swiss roll manifold using maximum variance unfolding.

Now, in the feature space $\mathcal{H}$, consider a kernel operator K_p as (Williams & Seeger, 2000), (Bengio et al., 2003a, Section 3):

$$(K_p f)(\boldsymbol{x}) := \int k(\boldsymbol{x}, \boldsymbol{y})\, f(\boldsymbol{y})\, p(\boldsymbol{y})\, d\boldsymbol{y}, \qquad (3)$$

where $f \in \mathcal{H}$ and the density function $p(\boldsymbol{y})$ can be approximated empirically. The eigenfunction problem for this kernel operator is (Ghojogh et al., 2021b):

$$(K_p f_k)(\boldsymbol{x}) = \lambda_k f_k(\boldsymbol{x}), \quad \forall k \in \{1, \ldots, n\}, \qquad (4)$$

where $f_k(.)$ is the k-th eigenfunction and λ_k is the corresponding eigenvalue.

Lemma 1 (Relation of Eigenfunctions and Eigenvectors for Kernel (Bengio et al., 2003a, Proposition 1), (Bengio et al., 2003c, Theorem 1))**.** *Consider a training dataset $\{\boldsymbol{x}_i \in \mathbb{R}^d\}_{i=1}^n$ and the eigenvalue problem (1) where $\boldsymbol{v}_k \in \mathbb{R}^n$ and δ_k are the k-th eigenvector and eigenvalue of matrix $\boldsymbol{K} \in \mathbb{R}^{n \times n}$. If v_{ki} is the i-th element of vector $\boldsymbol{v}_k$, the eigenfunction for the point $\boldsymbol{x}$ and the i-th training point $\boldsymbol{x}_i$ are:*

$$f_k(\boldsymbol{x}) = \frac{\sqrt{n}}{\delta_k} \sum_{i=1}^{n} v_{ki}\, \breve{k}(\boldsymbol{x}_i, \boldsymbol{x}), \qquad (5)$$

$$f_k(\boldsymbol{x}_i) = \sqrt{n}\, v_{ki}, \qquad (6)$$

respectively, where $\breve{k}(\boldsymbol{x}_i, \boldsymbol{x})$ is the centered kernel. If $\boldsymbol{x}$ is a training point, $\breve{k}(\boldsymbol{x}_i, \boldsymbol{x})$ is the centered kernel over training data and if $\boldsymbol{x}$ is an out-of-sample point, then $\breve{k}(\boldsymbol{x}_i, \boldsymbol{x}) = \breve{k}_t(\boldsymbol{x}_i, \boldsymbol{x})$ is between training set and the out-of-sample point (n.b. see (Ghojogh et al., 2021b) for information on kernel centering).

Theorem 1 (Embedding from Eigenfunctions of Kernel Operator (Bengio et al., 2003a, Proposition 1), (Bengio et al., 2003c, Section 4))**.** *Consider a dimensionality reduction algorithm which embeds data into a low-dimensional embedding space. Let the embedding of the point $\boldsymbol{x}$ be $\mathbb{R}^p \ni \boldsymbol{y}(\boldsymbol{x}) = [y_1(\boldsymbol{x}), \ldots, y_p(\boldsymbol{x})]^\top$ where $p \leq n$. The k-th dimension of this embedding is:*

$$y_k(\boldsymbol{x}) = \sqrt{\delta_k}\, \frac{f_k(\boldsymbol{x})}{\sqrt{n}} = \frac{1}{\sqrt{\delta_k}} \sum_{i=1}^{n} v_{ki}\, \breve{k}(\boldsymbol{x}_i, \boldsymbol{x}), \quad (7)$$

where $\breve{k}(\boldsymbol{x}_i, \boldsymbol{x})$ is the centered training or out-of-sample kernel depending on whether $\boldsymbol{x}$ is a training or an out-of-sample point.

The Theorem 1 has been widely used for out-of-sample (test data) embedding in many spectral dimensionality reduction algorithms (Bengio et al., 2003a). This theorem also explains why spectral methods can all be seen as kernel PCA for learning eigenfunctions. In the following, we justify this insight into unification of the spectral methods.

2.2. Unified Framework as Kernel PCA

Many spectral dimensionality reduction methods can be reduced to kernel PCA where the eigenvectors of the kernel matrix or eigenfunctions of the kernel operator are used for embedding as was stated in Lemma 1 and Theorem 1. This unification was analyzed in the following two categories of papers:

- papers for eigenfunction learning: (Bengio et al., 2003b;c;a; 2004; 2006)

- papers for unification by kernels constructed from distance matrices: (Ham et al., 2004) and (Strange & Zwiggelaar, 2014, Table 2.1) and (Ghojogh et al., 2019b)

In the following, we explain this unification of spectral methods as kernel PCA using both approaches together.

– Principal Component analysis (PCA):

As kernel PCA makes use of kernel trick for kernelization, it is equivalent to PCA when a linear kernel is used (Ghojogh et al., 2021b). Hence, PCA (Ghojogh & Crowley, 2019) is equivalent to kernel PCA by the linear kernel:

$$\boldsymbol{K} = \boldsymbol{X}^\top \boldsymbol{X}. \qquad (8)$$

– Multidimensional Scaling (MDS):

According to our derivations in (Ghojogh et al., 2020b) or (Ghojogh et al., 2021b), MDS (Cox & Cox, 2008) is equivalent to kernel PCA with the kernel:

$$\boldsymbol{K} = -\frac{1}{2} \boldsymbol{H} \boldsymbol{D} \boldsymbol{H}, \qquad (9)$$

where $\boldsymbol{D}$ is the squared Euclidean distance matrix and $\boldsymbol{H} := \boldsymbol{I} - (1/n)\boldsymbol{1}\boldsymbol{1}^\top$ is the centering matrix.

– Spectral Clustering:

Let $\boldsymbol{W} \in \mathbb{R}^{n \times n}$ be the adjacency matrix of points (Ghojogh et al., 2021a). Spectral clustering (Weiss, 1999; Ng

et al., 2001; Ghojogh et al., 2021a) uses the normalized adjacency matrix as its kernel matrix. Suppose $\boldsymbol{D}_{i,i} := \sum_{j=1}^{n} \boldsymbol{W}_{ij}$ is the (i, i)-th element of the diagonal degree matrix of adjacency matrix. Hence, the (i, j)-th element of kernel is (Weiss, 1999; Bengio et al., 2003a):

$$\boldsymbol{K}_{ij} = \frac{\boldsymbol{W}_{ij}}{\sqrt{\boldsymbol{D}_{ii}\,\boldsymbol{D}_{jj}}}, \qquad (10)$$

where $\boldsymbol{K}_{ij} = k(\boldsymbol{x}_i, \boldsymbol{x}_j)$ for the kernel function $k(.,.)$. This relation of kernel matrix with the adjacency matrix makes sense because kernel is a notion of similarity (Ghojogh et al., 2021b).

– Laplacian Eigenmap:

The solution of Laplacian eigenmap (Belkin & Niyogi, 2001; Ghojogh et al., 2021a) is the generalized eigenvalue problem $(\boldsymbol{L}, \boldsymbol{D})$ (Ghojogh et al., 2019a) where $\boldsymbol{L} := \boldsymbol{D} - \boldsymbol{W}$ is the Laplacian of the adjacency matrix $\boldsymbol{W}$. According to (Weiss, 1999, Normalization Lemma 1) , the eigenvectors of the generalized eigenvalue problem $(\boldsymbol{L}, \boldsymbol{D})$ are equivalent to the eigenvectors of the normalized kernel in Eq. (10).

In addition to the above analysis (Bengio et al., 2003a), there exists another analysis for Laplacian eigenmap stated in (Ham et al., 2004). Consider the Laplacian of graph of data. It can, for example, be the Laplacian of RBF adjacency matrix. It was mentioned above that the solution of Laplacian eigenmap is the generalized eigenvalue problem $(\boldsymbol{L}, \boldsymbol{D})$. However, there exists another form of optimization for Laplacian eigenmap whose solution is the eigenvalue problem for $\boldsymbol{L}$ (Ghojogh et al., 2021a). As the optimization of Laplacian eigenmap is minimization, its eigenvectors are sorted from the smallest to largest eigenvalues (Ghojogh et al., 2019a). However, the optimization in PCA and kernel PCA is maximization and the eigenvectors are sorted from the largest to smallest eigenvalues. Hence, to have equivalency with kernel PCA, we should modify minimization to maximization. One way to do this is to replace $\boldsymbol{L}$ with (Ham et al., 2004):

$$\mathbb{R}^{n \times n} \ni \boldsymbol{K} = \boldsymbol{L}^{\dagger}, \qquad (11)$$

where † denotes the pseudo-inverse of matrix. This replacement changes minimization to maximization because the Laplacian matrix is positive semidefinite (Ghojogh et al., 2021a) and eigenvalues of inverse of a positive semidefinite matrix are equivalent to the reciprocal of eigenvalues that matrix while the eigenvectors remain the same. Hence, the order of eigenvalues and eigenvectors become reversed. It is also important that the pseudo-inverse of Laplacian used as the kernel should be double-centered because kernel is double-centered in kernel PCA (Ghojogh & Crowley, 2019). It is interesting that Eq. (11) is already double-

centered (Ham et al., 2004):

$$\boldsymbol{L}\mathbf{1} = \boldsymbol{L}^{\dagger}\mathbf{1} = \mathbf{0} \implies \boldsymbol{H}\boldsymbol{L}^{\dagger}\boldsymbol{H} = \boldsymbol{L}^{\dagger},$$

where $\boldsymbol{H} := \boldsymbol{I} - (1/n)\mathbf{1}\mathbf{1}^{\top}$ is the centering matrix. Note that $\boldsymbol{L}\mathbf{1} = \boldsymbol{L}^{\dagger}\mathbf{1} = \mathbf{0}$ holds because the row summation of Laplacian matrix is zero (Ghojogh et al., 2021a).

– Isomap:

The kernel in Isomap is (Tenenbaum et al., 2000; Ghojogh et al., 2020b):

$$\boldsymbol{K} = -\frac{1}{2}\boldsymbol{H}\boldsymbol{D}^{(g)}\boldsymbol{H}, \qquad (12)$$

where $\boldsymbol{D}^{(g)}$ is the geodesic distance matrix whose elements are the (squared) approximation of geodesic distances using piece-wise Euclidean distances (Ghojogh et al., 2020b). Hence, it can be seen as kernel PCA with the above-mentioned kernel (Ham et al., 2004).

– Locally Linear Embedding (LLE):

The solution of LLE is the eigenvectors of $\boldsymbol{M} := (\boldsymbol{I} - \boldsymbol{W})^{\top}(\boldsymbol{I} - \boldsymbol{W})$ where $\boldsymbol{I}$ is the identity matrix and $\boldsymbol{W}$ is the weight matrix obtained from the linear reconstruction step in LLE (Roweis & Saul, 2000; Ghojogh et al., 2020a). As the optimization of LLE is minimization, its eigenvalues are sorted from smallest to largest (Ghojogh et al., 2019a). However, PCA and kernel PCA have maximization in their formulation. Hence, to have equivalency with kernel PCA, we should modify minimization to maximization. One way to do this is to replace $\boldsymbol{M}$ with (Schölkopf et al., 2002; Bengio et al., 2003b):

$$\mathbb{R}^{n \times n} \ni \boldsymbol{K} = \mu\boldsymbol{I} - \boldsymbol{M}, \qquad (13)$$

where $\mu > 0$. It is suggested in (Ham et al., 2004) to set μ to the largest eigenvalue $\lambda_{\max}$ of $\boldsymbol{M}$ so that the kernel $\boldsymbol{K}$ becomes positive definite. This replacement of $\boldsymbol{M}$ with the provided kernel changes minimization to maximization because:

$$\arg\max(\boldsymbol{K}) \overset{(13)}{=} \arg\max(-\boldsymbol{M}) = \arg\min(\boldsymbol{M}).$$

Another possible replacement exists and that is replacing $\boldsymbol{M}$ with its pseudo-inverse (Alipanahi & Ghodsi, 2011, Section 2.1):

$$\mathbb{R}^{n \times n} \ni \boldsymbol{K} = \boldsymbol{M}^{\dagger}, \qquad (14)$$

whose justification is similar to justification of pseudo-inverse of Laplacian for Laplacian eigenmap.

– Diffusion Map:

Diffusion map (Coifman & Lafon, 2006) is a Laplacian-based method (Ghojogh et al., 2021a) and can be seen as

Table 1. The summary of kernels for unification of spectral methods as kernel PCA

Method	Kernel
PCA	$\boldsymbol{X}^\top \boldsymbol{X}$
MDS	$-\frac{1}{2}\boldsymbol{HDH}$
Spectral clustering	$\frac{\boldsymbol{W}_{ij}}{\sqrt{\boldsymbol{D}_{ii}\boldsymbol{D}_{jj}}}$
Laplacian eigenmap	$\boldsymbol{L}^\dagger$ or $\frac{\boldsymbol{W}_{ij}}{\sqrt{\boldsymbol{D}_{ii}\boldsymbol{D}_{jj}}}$
Isomap	$-\frac{1}{2}\boldsymbol{HD}^{(g)}\boldsymbol{H}$
LLE	$\boldsymbol{M}^\dagger$ or $\lambda_{\max}\boldsymbol{I} - \boldsymbol{M}$
Diffusion map	$\boldsymbol{M}^t$

a special case of kernel PCA with a specific kernel (Ham et al., 2004), (Strange & Zwiggelaar, 2014, Chapter 2). Let $\boldsymbol{M}$ denote the random-walk graph Laplacian normalization of Laplacian, i.e., $\boldsymbol{M} := (\boldsymbol{D}^{(\alpha)})^{-1}\boldsymbol{L}^{(\alpha)}$ where α is a parameter. At time t, we can say that $\boldsymbol{M}^t$ is the probability of going from $\boldsymbol{x}_i$ to $\boldsymbol{x}_j$. The solution of diffusion map at time t is the eigenvectors of $\boldsymbol{M}^t$ sorted from largest to smallest eigenvalues (Ghojogh et al., 2021a). Hence, we can consider the following kernel for equivalency of diffusion map and kernel PCA:

$$\mathbb{R}^{n\times n} \ni \boldsymbol{K} = \boldsymbol{M}^t, \tag{15}$$

because kernel PCA also has maximization in its formulation.

2.3. Summary of Kernels in Spectral Methods
As we saw, kernels in some algorithms such as PCA and MDS are almost closed-form and can be computed almost fast. However, some methods such as Isomap require a piece of code to calculate their kernels. We can have a summary of kernels for unification of spectral dimensionality reduction methods as kernel PCA. A similar summary exists in (Strange & Zwiggelaar, 2014, Table 2.1). We summarize the kernels in Table 1.

2.4. Generalized Embedding
It was demonstrated above that many of the spectral dimensionality reduction methods belong to a unified framework. Therefore, there can be generalized embedding methods which generalize the spectral methods to broader algorithms. Graph Embedding (GE) (Yan et al., 2005; 2006; Ghojogh et al., 2021a) showed that many spectral methods, including Laplacian eigenmap, locality preserving projection, PCA and kernel PCA, Fisher Discriminant Analysis (FDA) and kernel FDA, MDS, Isomap, and LLE, are special cases of a model named graph embedding. Another generalized subspace learning method, named Roweis Dis-

criminant Analysis (RDA), also generalized PCA, supervised PCA, and FDA as unified methods. These generalized methods justify from another perspective that why spectral methods can be unified.

3. Background on Semidefinite Programming
Here, we review some optimization background required for solving SDP used in MVU and kernel learning.

3.1. Unconstrained Optimization
Consider the following optimization problem:

$$\underset{\boldsymbol{x}}{\text{minimize}} \quad f(\boldsymbol{x}). \tag{16}$$

where $f(.)$ is a convex function. Iterative optimization can be first-order or second-order. Iterative optimization updates solution iteratively:

$$\boldsymbol{x} \leftarrow \boldsymbol{x} + \Delta\boldsymbol{x}, \tag{17}$$

until $\Delta\boldsymbol{x}$ becomes very small which is the convergence of optimization. In the first-order optimization, the step of updating is $\Delta\boldsymbol{x} := -\nabla f(\boldsymbol{x})$ where $\nabla f(.)$ denotes the gradient of function. Near the optimal point $\boldsymbol{x}^*$, gradient is very small so the second-order Taylor series expansion of function becomes:

$$f(\boldsymbol{x}) \approx f(\boldsymbol{x}^*) + \underbrace{\nabla f(\boldsymbol{x}^*)^\top}_{\approx 0}(\boldsymbol{x} - \boldsymbol{x}^*)$$
$$+ \frac{1}{2}(\boldsymbol{x} - \boldsymbol{x}^*)^\top \nabla^2 f(\boldsymbol{x}^*)(\boldsymbol{x} - \boldsymbol{x}^*)$$
$$\approx f(\boldsymbol{x}^*) + \frac{1}{2}(\boldsymbol{x} - \boldsymbol{x}^*)^\top \nabla^2 f(\boldsymbol{x}^*)(\boldsymbol{x} - \boldsymbol{x}^*),$$

where $\nabla^2 f(\boldsymbol{x})$ denotes the second-order gradient (Hessian) of function. This shows that the function is almost quadratic near the optimal point. Following this intuition, Newton's method uses Hessian $\nabla^2 f(\boldsymbol{x})$ in its updating step:

$$\Delta\boldsymbol{x} := -\nabla^2 f(\boldsymbol{x})^{-1}\nabla f(\boldsymbol{x}). \tag{18}$$

3.2. Equality Constrained Optimization
The optimization problem may have equality constraint:

$$\underset{\boldsymbol{x}}{\text{minimize}} \quad f(\boldsymbol{x})$$
$$\text{subject to} \quad \boldsymbol{Ax} = \boldsymbol{b}. \tag{19}$$

After a step of update by $\Delta\boldsymbol{x} = \boldsymbol{u}$, this optimization becomes:

$$\underset{\boldsymbol{x}}{\text{minimize}} \quad f(\boldsymbol{x} + \boldsymbol{u})$$
$$\text{subject to} \quad \boldsymbol{A}(\boldsymbol{x} + \boldsymbol{u}) = \boldsymbol{b}. \tag{20}$$

The Lagrangian of this optimization problem is (Boyd et al., 2004):

$$\mathcal{L} = f(\boldsymbol{x} + \boldsymbol{u}) + \boldsymbol{\nu}^\top(\boldsymbol{A}(\boldsymbol{x} + \boldsymbol{u}) - \boldsymbol{b}),$$

where $\boldsymbol{\nu}$ is the dual variable. The second-order Taylor series expansion of function $f(\boldsymbol{x} + \boldsymbol{u})$ is:

$$f(\boldsymbol{x} + \boldsymbol{u}) \approx f(\boldsymbol{x}) + \nabla f(\boldsymbol{x})^\top \boldsymbol{u} + \frac{1}{2} \boldsymbol{u}^\top \nabla^2 f(\boldsymbol{x}^*)\, \boldsymbol{u}. \tag{21}$$

Substituting this into the Lagrangian gives:

$$\begin{aligned}
\mathcal{L} = &\, f(\boldsymbol{x}) + \nabla f(\boldsymbol{x})^\top \boldsymbol{u} + \frac{1}{2} \boldsymbol{u}^\top \nabla^2 f(\boldsymbol{x}^*)\, \boldsymbol{u} \\
&+ \boldsymbol{\nu}^\top (\boldsymbol{A}(\boldsymbol{x} + \boldsymbol{u}) - \boldsymbol{b}).
\end{aligned}$$

According to Karush–Kuhn–Tucker (KKT) conditions, the primal and dual residuals must be zero:

$$\nabla_{\boldsymbol{x}} \mathcal{L} = \nabla f(\boldsymbol{x}) + \nabla^2 f(\boldsymbol{x})^\top \boldsymbol{u} + \boldsymbol{u}^\top \underbrace{\nabla^3 f(\boldsymbol{x}^*)}_{\approx\, \boldsymbol{0}}\, \boldsymbol{u}$$

$$+ \boldsymbol{A}^\top \boldsymbol{\nu} \overset{\text{set}}{=} \boldsymbol{0} \implies \nabla^2 f(\boldsymbol{x})^\top \boldsymbol{u} + \boldsymbol{A}^\top \boldsymbol{\nu} = -\nabla f(\boldsymbol{x}), \tag{22}$$

$$\nabla_{\boldsymbol{\nu}} \mathcal{L} = \boldsymbol{A}(\boldsymbol{x} + \boldsymbol{u}) - \boldsymbol{b} \overset{(a)}{=} \boldsymbol{A} \boldsymbol{u} \overset{\text{set}}{=} \boldsymbol{0}, \tag{23}$$

where we have $\nabla^3 f(\boldsymbol{x}^*) \approx 0$ because the gradient of function at the optimal point vanishes and (a) is because of the constraint $\boldsymbol{A}\boldsymbol{x} - \boldsymbol{b} = \boldsymbol{0}$ in problem (19). Eqs. (22) and (23) can be written as a system of equations:

$$\begin{bmatrix} \nabla^2 f(\boldsymbol{x})^\top & \boldsymbol{A}^\top \\ \boldsymbol{A} & \boldsymbol{0} \end{bmatrix} \begin{bmatrix} \boldsymbol{u} \\ \boldsymbol{\nu} \end{bmatrix} = \begin{bmatrix} -\nabla f(\boldsymbol{x}) \\ \boldsymbol{0} \end{bmatrix}. \tag{24}$$

Solving this system of equations gives the desired step $\boldsymbol{u}$ for updating the solution at the iteration.

3.3. Inequality Constrained Optimization

The optimization problem may have equality constraint:

$$\begin{aligned}
&\underset{\boldsymbol{x}}{\text{minimize}} && f(\boldsymbol{x}) \\
&\text{subject to} && f_i(\boldsymbol{x}) \leq 0, \quad i \in \{1, \dots, m\}, \\
& && \boldsymbol{A}\boldsymbol{x} = \boldsymbol{b}.
\end{aligned} \tag{25}$$

Barrier methods, also known as interior-point methods, convert inequality constrained problems to equality constrained or unconstrained problems. Ideally, we can do this conversion using the indicator function $\mathbb{I}(.)$ which is zero if its input condition is satisfied and is infinity otherwise (n.b. the indicator function in optimization literature is not like the indicator in data science which is one if its input condition is satisfied and is zero otherwise). The problem is converted to:

$$\begin{aligned}
&\underset{\boldsymbol{x}}{\text{minimize}} && f(\boldsymbol{x}) + \sum_{i=1}^{m} \mathbb{I}(f_i(\boldsymbol{x}) \leq 0) \\
&\text{subject to} && \boldsymbol{A}\boldsymbol{x} = \boldsymbol{b}.
\end{aligned} \tag{26}$$

The indicator function is not differentiable because it is not smooth. Hence, we can approximate it with differentiable functions such as logarithm. Logarithmic barrier approximates the indicator function by:

$$\mathbb{I}(f_i(\boldsymbol{x}) \leq 0) \approx -\frac{1}{t} \log(-f_i(\boldsymbol{x})), \tag{27}$$

where the approximation becomes more accurate by $t \to \infty$. It changes the problem to:

$$\begin{aligned}
&\underset{\boldsymbol{x}}{\text{minimize}} && f(\boldsymbol{x}) - \frac{1}{t} \sum_{i=1}^{m} \log(-f_i(\boldsymbol{x})) \\
&\text{subject to} && \boldsymbol{A}\boldsymbol{x} = \boldsymbol{b}.
\end{aligned} \tag{28}$$

This optimization problem is an equality constrained optimization problem which we already explained how to solve.

3.4. Semidefinite Programming

An optimization problem in the following form is a Semidefinite Programming (SDP) (Vandenberghe & Boyd, 1996):

$$\begin{aligned}
&\underset{\boldsymbol{X}}{\text{minimize}} && \mathbf{tr}(\boldsymbol{C}^\top \boldsymbol{X}) \\
&\text{subject to} && \mathbf{tr}(\boldsymbol{A}_i^\top \boldsymbol{X}) = \boldsymbol{b}_i, \quad i \in \{1, \dots, m_1\}, \\
& && \mathbf{tr}(\boldsymbol{D}_i^\top \boldsymbol{X}) \leq \boldsymbol{e}_i, \quad i \in \{1, \dots, m_2\}, \\
& && \boldsymbol{X} \succeq \boldsymbol{0},
\end{aligned} \tag{29}$$

where $\boldsymbol{C}$, $\boldsymbol{A}_i$'s, and $\boldsymbol{D}_i$'s are constant matrices and $\boldsymbol{b}_i$'s and $\boldsymbol{e}_i$'s are constant vectors. Note that the trace terms may be written in summation forms. The interior-point method, or the barrier method, introduced before, can be used for solving SDP (Nesterov & Nemirovskii, 1994; Boyd et al., 2004). Optimization toolboxes such as CVX (Grant et al., 2008) often use interior-point method for solving optimization problems such as SDP. Note that this method is iterative and SDP solving usually is time consuming especially for large matrices. Also note that SDP is a convex optimization problem so it has only one local optimum which is the global optimum (Boyd et al., 2004).

4. Kernel Learning for Transduction

Kernel learning by semidefinite programming was initially proposed in (Lanckriet et al., 2004) for the goal of transduction. Transduction is a task in which the labeling of a not-completely-labeled dataset gets complete. In other words, using the labeled part of data, the embedding for the unlabeled part of data is also calculated. It seems that the paper (Lanckriet et al., 2004) has inspired the authors of MVU or SDE (Weinberger et al., 2004) to use semidefinite programming in kernel learning for the task of dimensionality reduction. As kernel learning for transduction is not completely related to dimensionality reduction, we briefly introduce it and do not enter its details. The reader can refer to (Lanckriet et al., 2004) or its summary in (Karimi, 2017) for more information about it.

Consider a dataset which is partially labeled. The labeled and unlabeled sets of data can be the training and test sets, respectively. Let the training and test sets be denoted by $\{(\boldsymbol{x}_i, y_i)\}_{i=1}^{n_{\text{tr}}}$ and $\{\boldsymbol{x}_i\}_{i=n_{\text{tr}}+1}^{n_{\text{te}}}$, respectively, where n_{tr} is the number of labeled training points and n_{te} is the number of unlabeled test points and $n := n_{\text{tr}} + n_{\text{te}}$. The kernel matrix has the following sub-matrices:

$$\mathbb{R}^{n \times n} \ni \boldsymbol{K} = \begin{bmatrix} \boldsymbol{K}_{\text{tr,tr}} & \boldsymbol{K}_{\text{tr,te}} \\ \boldsymbol{K}_{\text{te,tr}} & \boldsymbol{K}_{\text{te,te,}} \end{bmatrix}, \qquad (30)$$

where $\boldsymbol{K}_{\text{tr,tr}} \in \mathbb{R}^{n_{\text{tr}} \times n_{\text{tr}}}$, $\boldsymbol{K}_{\text{tr,te}} \in \mathbb{R}^{n_{\text{tr}} \times n_{\text{te}}}$, $\boldsymbol{K}_{\text{te,tr}} \in \mathbb{R}^{n_{\text{te}} \times n_{\text{tr}}}$, and $\boldsymbol{K}_{\text{te,te}} \in \mathbb{R}^{n_{\text{te}} \times n_{\text{te}}}$. We will see later that MVU (Weinberger et al., 2004) learns the best kernel matrix for manifold unfolding. However, in contrast to kernel learning in MVU which learns the kernel matrix by optimization, the kernel learning proposed in (Lanckriet et al., 2004) finds the best kernel among a set of available kernels. Let $\mathcal{K} := \{\boldsymbol{K}_1, \ldots, \boldsymbol{K}_m\}$ be the set of kernels whose elements can be different kernels such as linear kernel, RBF kernel, Laplacian kernel, etc (Ghojogh et al., 2021b). Kernel learning in this section learns the best kernel as one of the kernels in the set.

We can learn the kernel among the sets of kernels by the following optimization problem (Lanckriet et al., 2004, Theorem 16):

$$\begin{aligned} \underset{\boldsymbol{K}, \boldsymbol{\nu}, \boldsymbol{\delta}, \lambda, t}{\text{minimize}} \quad & t \\ \text{subject to} \quad & \mathbf{tr}(\boldsymbol{K}) = c_1, \\ & \boldsymbol{K} \in \mathcal{K}, \\ & \boldsymbol{\nu} \geq \mathbf{0}, \\ & \boldsymbol{\delta} \geq \mathbf{0}, \\ & \begin{bmatrix} G(\boldsymbol{K}_{\text{tr}}) + \tau \boldsymbol{I} & \mathbf{1} + \boldsymbol{\nu} - \boldsymbol{\delta} + \lambda \boldsymbol{y} \\ (\mathbf{1} + \boldsymbol{\nu} - \boldsymbol{\delta} + \lambda \boldsymbol{y})^\top & t - 2 c_2 \boldsymbol{\delta}^\top \mathbf{1} \end{bmatrix} \succeq \mathbf{0}, \end{aligned}$$
$$(31)$$

where c_1, c_2, and τ are constants, and the (i,j)-th element of $G(\boldsymbol{K}_{\text{tr}})$ is defined as $G_{ij}(\boldsymbol{K}_{\text{tr}}) := y_i y_j \boldsymbol{K}_{ij}$. Note that $\boldsymbol{K}_{ij}$ is the (i,j)-th element of the kernel matrix and we consider a binary classification here so the labels are $y_i \in \{-1, 1\}, \forall i$. The derivation of this problem is available in (Karimi, 2017, Appendix B). This optimization problem is in one of the forms of semidefinite programming problem (Vandenberghe & Boyd, 1996). See Section 3 for more information on semidefinite programming and how it is solved. As it is a SDP, it is a convex problem and has only one local optimum (Boyd et al., 2004).

After learning the kernel $\boldsymbol{K} \in \mathcal{K}$, it can be used for predicting the labels of unlabeled part of data, i.e., the test dataset. The paper (Lanckriet et al., 2004) uses kernel Support Vector Machine (SVM) (Vapnik, 1995) for predicting labels using the learned kernel. Using kernelization techniques (Ghojogh et al., 2021b), the predictor of labels in kernel SVM becomes:

$$f(\boldsymbol{x}) = \sum_{i=1}^{n} \alpha_i \, k(\boldsymbol{x}_i, \boldsymbol{x}) + b, \qquad (32)$$

where $k(.,.)$ is the kernel function (Ghojogh et al., 2021b) which determines the elements of the kernel matrix $\boldsymbol{K}_{ij} = k(\boldsymbol{x}_i, \boldsymbol{x}_j)$. Also, $\boldsymbol{\alpha} = [\alpha_1, \ldots, \alpha_n]^\top$ and b is the bias. By using the learned kernel $\boldsymbol{K}$ in Eq. (32), one can predict the labels of unlabeled test data. As was mentioned before, this kernel learning may have inspired the authors of MVU or SDE (Weinberger et al., 2004) to propose kernel learning for dimensionality reduction.

5. Maximum Variance Unfolding (or Semidefinite Embedding)

Kernel can be learned using SDP for the sake of dimensionality reduction and manifold unfolding. In the following, we introduce kernel learning using SDP for this goal.

5.1. Intuitions and Comparison with Kernel PCA

As we saw in Section 2, most of the spectral dimensionality reduction methods can be unified as kernel PCA with different kernels. Therefore, let us learn the best kernel in dimensionality reduction for every specific dataset.

Semidefinite Embedding (SDE) (Weinberger et al., 2004; Weinberger & Saul, 2004; Weinberger et al., 2005; Weinberger & Saul, 2006b), which was renamed later to Maximum Variance Unfolding (MVU) (Weinberger & Saul, 2006a), aims to find the best kernel which unfolds the manifold of data to its maximum variance. It learns the best kernel for manifold unfolding using semidefinite programming. An example manifold unfolding is shown in Fig. 2 where MVU gradually unfolds the nonlinear manifold to its extreme variance by iterations of semidefinite programming.

By MVU, the embedding of data has its maximum variance in the embedding space. In this sense, the goal is similar to the goal of PCA (Ghojogh & Crowley, 2019) but there are major differences between MVU and PCA and kernel PCA. Some differences and similarities are:

- MVU performs embedding in the feature space or the so-called Reproducing Kernel Hilbert Space (RKHS); so does kernel PCA. However, PCA performs in the input space.

- MVU learns the best kernel while kernel PCA uses a ready kernel such as the Radial Basis Function (RBF) kernel.

- MVU is a nonlinear method. Kernel PCA transforms data to the feature space and then applies linear PCA to it. See (Ghojogh et al., 2021b) for more explanation on the difference of these two approaches.

- MVU is an iterative algorithm because it solves semidefinite programming iteratively (see Section 3). However, kernel PCA and PCA are almost closed form. We use the word "almost" because solving the eigenvalue decomposition (EVD) or singular value decomposition (SVD) requires some iterations by algorithms such as the power method or Jordan's method (Stewart, 1993) but we can see the solution of EVD or SVD as a black box. The iterative solution of semidefinite programming in MVU is much more complicated and time consuming although the task done by MVU is more promising in manifold unfolding.

Assume we have a d-dimensional dataset $\mathcal{X} := \{\boldsymbol{x}_i \in \mathbb{R}^d\}_{i=1}^n$. We aim to find a p-dimensional embedding of this dataset, denoted by $\mathcal{Y} := \{\boldsymbol{y}_i \in \mathbb{R}^p\}_{i=1}^n$ where $p \leq d$ and usually $p \ll d$. Let $\boldsymbol{X} := [\boldsymbol{x}_1, \ldots, \boldsymbol{x}_n] \in \mathbb{R}^{d \times n}$ and $\boldsymbol{Y} := [\boldsymbol{y}_1, \ldots, \boldsymbol{y}_n] \in \mathbb{R}^{p \times n}$. The embedding $\boldsymbol{Y}$ is supposed to be the maximum variance unfolding of the manifold of data. As mentioned before, SDE (Weinberger et al., 2004; Weinberger & Saul, 2004; Weinberger et al., 2005; Weinberger & Saul, 2006b) or MVU (Weinberger & Saul, 2006a) performs this task. MVU embeds data in the feature space or RKHS; in other words, the embedding space is the feature space (RKHS). Hence:

$$\boldsymbol{y}_i = \boldsymbol{\phi}(\boldsymbol{x}_i), \quad \forall i \in \{1, \ldots, n\}. \tag{33}$$

5.2. Local Isometry

Definition 2 (Isometric Manifolds (Weinberger & Saul, 2004)). *Two Riemannian manifolds are isometric if there is a diffeomorphism such that the metric on one of them pulls back to the metric on the other one. In other words, isometry is is a smooth invertible mapping which locally looks like an affine transformation, i.e., a rotation and a translation. Hence, isometry preserves the local distances on the manifold.*

We use the notion of isometry between the data $\mathcal{X}$ and their embedding $\mathcal{Y}$. In other words, the local structure of data should be preserved in the embedding space (Saul & Roweis, 2003). The datasets $\mathcal{X}$ and $\mathcal{Y}$ are locally isometric if they have similar rotation and translation relations between neighbor points. Let $\boldsymbol{x}_j$ and $\boldsymbol{x}_l$ be neighbors of $\boldsymbol{x}_i$ so that they form a triangle. This triangle should also exist in the low dimensional embedding space with some rotation and translation. Hence, for isometry, we should have equal relative angles of points:

$$(\boldsymbol{y}_i - \boldsymbol{y}_j)^\top (\boldsymbol{y}_i - \boldsymbol{y}_l) = (\boldsymbol{x}_i - \boldsymbol{x}_j)^\top (\boldsymbol{x}_i - \boldsymbol{x}_l), \tag{34}$$

because inner product is proportional to the cosine of angle. A special case of Eq. (34) is $l = j$:

$$\|\boldsymbol{y}_i - \boldsymbol{y}_j\|_2^2 = \|\boldsymbol{x}_i - \boldsymbol{x}_j\|_2^2. \tag{35}$$

We denote the Gram (kernel) matrices of points in the input and embedding spaces by $\mathbb{R}^{n \times n} \ni \boldsymbol{G} := \boldsymbol{X}^\top \boldsymbol{X}$ and $\mathbb{R}^{n \times n} \ni \boldsymbol{K} := \boldsymbol{Y}^\top \boldsymbol{Y}$, respectively. Let $\boldsymbol{G}_{ij}$ and $\boldsymbol{K}_{ij}$ denote the (i, j)-th element of $\boldsymbol{G}$ and $\boldsymbol{K}$, respectively. We have:

$$\|\boldsymbol{x}_i - \boldsymbol{x}_j\|_2^2 = (\boldsymbol{x}_i - \boldsymbol{x}_j)^\top (\boldsymbol{x}_i - \boldsymbol{x}_j)$$
$$= \boldsymbol{x}_i^\top \boldsymbol{x}_i + \boldsymbol{x}_j^\top \boldsymbol{x}_j - 2\,\boldsymbol{x}_i^\top \boldsymbol{x}_j = \boldsymbol{G}_{ii} + \boldsymbol{G}_{jj} - 2\,\boldsymbol{G}_{ij}.$$

Likewise, in the embedding space we have:

$$\|\boldsymbol{y}_i - \boldsymbol{y}_j\|_2^2 = (\boldsymbol{y}_i - \boldsymbol{y}_j)^\top (\boldsymbol{y}_i - \boldsymbol{y}_j)$$
$$= \boldsymbol{y}_i^\top \boldsymbol{y}_i + \boldsymbol{y}_j^\top \boldsymbol{y}_j - 2\,\boldsymbol{y}_i^\top \boldsymbol{y}_j$$
$$\overset{(33)}{=} \boldsymbol{\phi}(\boldsymbol{x}_i)^\top \boldsymbol{\phi}(\boldsymbol{x}_i) + \boldsymbol{\phi}(\boldsymbol{x}_j)^\top \boldsymbol{\phi}(\boldsymbol{x}_j) - 2\,\boldsymbol{\phi}(\boldsymbol{x}_i)^\top \boldsymbol{\phi}(\boldsymbol{x}_j)$$
$$\overset{(a)}{=} \boldsymbol{K}_{ii} + \boldsymbol{K}_{jj} - 2\,\boldsymbol{K}_{ij}, \tag{36}$$

where (a) is because of kernel trick (Ghojogh et al., 2021b). Note that Eq. (36) is in fact the distance of points in RKHS equipped with kernel k (Schölkopf, 2001; Ghojogh et al., 2021b):

$$\|\boldsymbol{y}_i - \boldsymbol{y}_j\|_2^2 \overset{(33)}{=} \|\boldsymbol{\phi}(\boldsymbol{x}_i) - \boldsymbol{\phi}(\boldsymbol{x}_j)\|_k^2 = \boldsymbol{K}_{ii} + \boldsymbol{K}_{jj} - 2\boldsymbol{K}_{ij}.$$

Therefore, Eq. (35) is simplified to:

$$\boldsymbol{K}_{ii} + \boldsymbol{K}_{jj} - 2\,\boldsymbol{K}_{ij} = \boldsymbol{G}_{ii} + \boldsymbol{G}_{jj} - 2\,\boldsymbol{G}_{ij}. \tag{37}$$

Some version of MVU uses k-Nearest Neighbors (kNN) in the local isometry (Weinberger et al., 2004). This version forms a kNN graph between points of training data points. Hence, we know the k neighbors of every point in the dataset. Let τ_{ij} be one if $\boldsymbol{x}_j$ is a neighbor of $\boldsymbol{x}_i$ and zero otherwise:

$$\tau_{ij} := \begin{cases} 1 & \boldsymbol{x}_j \in k\text{NN}(\boldsymbol{x}_i) \\ 0 & \text{Otherwise.} \end{cases} \tag{38}$$

Considering the neighboring points only to have local isometry modifies Eq. (37) slightly:

$$\tau_{ij}(\boldsymbol{K}_{ii} + \boldsymbol{K}_{jj} - 2\,\boldsymbol{K}_{ij}) = \tau_{ij}(\boldsymbol{G}_{ii} + \boldsymbol{G}_{jj} - 2\,\boldsymbol{G}_{ij}). \tag{39}$$

5.3. Centering

We also want the embeddings of points to have zero mean:

$$\sum_{i=1}^n \boldsymbol{y}_i = \boldsymbol{0}. \tag{40}$$

This removes the translational degree of freedom. According to Eq. (33), centered embedding data means centered pulled data in the feature space. According to (Ghojogh et al., 2021b), this is equivalent to double centering the kernel matrix, resulting in:

$$\frac{1}{n} \sum_{i=1}^n \sum_{j=1}^n \boldsymbol{K}_{ij} = \boldsymbol{0} \implies \sum_{i=1}^n \sum_{j=1}^n \boldsymbol{K}_{ij} = \boldsymbol{0}. \tag{41}$$

Another justification for this is as follows. From Eq. (40), we have:

$$\Big|\sum_{i=1}^{n} \boldsymbol{y}_i\Big|^2 = \sum_{i=1}^{n}\sum_{j=1}^{n} \boldsymbol{y}_i^{\top}\boldsymbol{y}_j \overset{(33)}{=} \sum_{i=1}^{n}\sum_{j=1}^{n} \phi(\boldsymbol{x}_i)^{\top}\phi(\boldsymbol{x}_j)$$
$$\overset{(a)}{=} \sum_{i=1}^{n}\sum_{j=1}^{n} \boldsymbol{K}_{ij} \overset{(40)}{=} \boldsymbol{0},$$

where (a) is because of the kernel trick (Ghojogh et al., 2021b).

5.4. Positive Semidefiniteness

As we saw so far, we are expressing embedding using kernels because we assumed the embedding space is the feature space. Therefore, optimization can be performed over the kernel matrix rather than the embedding points. However, a valid Mercer kernel should be symmetric and positive semidefinite (Ghojogh et al., 2021b). Hence, the kernel matrix should be constrained to belong to the cone of semidefinite matrices:

$$\boldsymbol{K} \in \mathbb{S}_+^n, \quad \text{or} \quad \boldsymbol{K} \succeq \boldsymbol{0}. \tag{42}$$

5.5. Manifold Unfolding

The goal of MVU is unfolding the manifold of data with its maximum variance, as shown in Fig. 2. According to the definition of variance, MVU maximizes the following quantitative:

$$\mathcal{T}(\boldsymbol{Y}) := \frac{1}{2n}\sum_{i=1}^{n}\sum_{j=1}^{n} \|\boldsymbol{y}_i - \boldsymbol{y}_j\|_2^2. \tag{43}$$

Lemma 2 (Boundedness of Variance of Embedding (Weinberger & Saul, 2006b)). *The value of $\mathcal{T}(\boldsymbol{Y})$ is bounded.*

Proof. Suppose $\eta_{ij} = 1$ if $\boldsymbol{x}_j$ is one of the k-nearest neighbors (kNN) of $\boldsymbol{x}_i$; otherwise, $\eta_{ij} = 0$. Let:

$$\tau := \max_{i,j}\Big(\eta_{ij}\|\boldsymbol{x}_i - \boldsymbol{x}_j\|_2\Big) \overset{(a)}{<} \infty, \tag{44}$$

where (a) is because $\|\boldsymbol{x}_i - \boldsymbol{x}_j\|_2 < \infty$. Assuming that the kNN graph is connected, the longest path is at most $n\tau$, i.e., $\|\boldsymbol{y}_i - \boldsymbol{y}_j\|_2 \leq n\tau$. Therefore, an upper bound on Eq. (43) is:

$$\mathcal{T}(\boldsymbol{Y}) \leq \frac{1}{2n}\sum_{i=1}^{n}\sum_{j=1}^{n}(n\tau)^2 = \frac{1}{2n}n^2(n\tau)^2 = \frac{n^3\tau^2}{2} \overset{(44)}{<} \infty.$$

Q.E.D. $\qquad\qquad\qquad\qquad\qquad\qquad\square$

According to Lemma 2, the variance of embedding is bounded so we can maximize it.

The Eq. (43) can be simplified as:

$$\mathcal{T}(\boldsymbol{Y}) := \frac{1}{2n}\sum_{i=1}^{n}\sum_{j=1}^{n} \|\boldsymbol{y}_i - \boldsymbol{y}_j\|_2^2$$
$$\overset{(36)}{=} \frac{1}{2n}\sum_{i=1}^{n}\sum_{j=1}^{n}(\boldsymbol{K}_{ii} + \boldsymbol{K}_{jj} - 2\boldsymbol{K}_{ij})$$
$$= \frac{1}{2n}\Big[\sum_{i=1}^{n}\boldsymbol{K}_{ii} + \sum_{j=1}^{n}\boldsymbol{K}_{jj} - 2\sum_{i=1}^{n}\sum_{j=1}^{n}\boldsymbol{K}_{ij}\Big]$$
$$\overset{(41)}{=} \frac{1}{2n}\Big[\sum_{i=1}^{n}\boldsymbol{K}_{ii} + \sum_{j=1}^{n}\boldsymbol{K}_{jj}\Big] = \frac{1}{2n}\Big[2\sum_{i=1}^{n}\boldsymbol{K}_{ii}\Big]$$
$$= \frac{1}{n}\sum_{i=1}^{n}\boldsymbol{K}_{ii} \propto \sum_{i=1}^{n}\boldsymbol{K}_{ii} \overset{(a)}{=} \mathbf{tr}(\boldsymbol{K}), \tag{45}$$

where $\mathbf{tr}(.)$ denotes the trace of matrix and (a) is because trace of a matrix is equivalent to the summation of its diagonal elements. The Eq. (45) makes sense because kernel is a measure of similarity of points (Ghojogh et al., 2021b) so it is related to the distance of points and the variance of unfolding.

In summary, MVU maximizes the variance of embedding, i.e. Eq. (45), with constraints of Eqs. (37), (41), and (42). Hence, it solves the following optimization problem:

$$\begin{aligned} \underset{\boldsymbol{K}}{\text{maximize}} \quad & \mathbf{tr}(\boldsymbol{K}) \\ \text{subject to} \quad & \boldsymbol{K}_{ii} + \boldsymbol{K}_{jj} - 2\boldsymbol{K}_{ij} = \boldsymbol{G}_{ii} + \boldsymbol{G}_{jj} - 2\boldsymbol{G}_{ij}, \\ & \qquad\qquad\qquad\qquad \forall i,j \in \{1,\ldots,n\}, \\ & \sum_{i=1}^{n}\sum_{j=1}^{n} \boldsymbol{K}_{ij} = 0, \\ & \boldsymbol{K} \succeq \boldsymbol{0}, \end{aligned} \tag{46}$$

which is a semidefinite programming problem (Vandenberghe & Boyd, 1996). See Section 3 for more information on semidefinite programming and how it is solved. It is valuable that Eq. (46) is a convex optimization problem so it has only one local optimum which is the global optimum (Boyd et al., 2004).

The Eq. (46) is using Eq. (37) for local isometry. Some versions of MVU use Eq. (39) as the local isometry constraint:

$$\begin{aligned} \underset{\boldsymbol{K}}{\text{maximize}} \quad & \mathbf{tr}(\boldsymbol{K}) \\ \text{subject to} \quad & \tau_{ij}(\boldsymbol{K}_{ii} + \boldsymbol{K}_{jj} - 2\boldsymbol{K}_{ij}) \\ & \qquad = \tau_{ij}(\boldsymbol{G}_{ii} + \boldsymbol{G}_{jj} - 2\boldsymbol{G}_{ij}), \\ & \qquad\qquad\qquad \forall i,j \in \{1,\ldots,n\}, \\ & \sum_{i=1}^{n}\sum_{j=1}^{n} \boldsymbol{K}_{ij} = 0, \\ & \boldsymbol{K} \succeq \boldsymbol{0}, \end{aligned} \tag{47}$$

Note that if we see the entire dataset as one class and set $k = n$, Eq. (47) becomes equivalent to Eq. (46). Using kNN in Eq. (47) makes optimization slightly more efficient and faster because it does not compute kernel between all points; although, computation of kNN graph can be time-consuming.

5.6. Spectral Embedding

After kernel is found by solving optimization (46), we calculate the eigenvalues and eigenvectors of the kernel (Ghojogh et al., 2019a) and then the embedding of every point is obtained by Eq. (48) in the following lemma. The obtained embedding dataset has the maximum variance in the embedding space. Note that for finding the intrinsic dimensionality of manifold, denoted by $p \leq n$, we sort the eigenvalues from largest to smallest and a huge gap between two successive eigenvalues shows a good cut-off for the number of required dimensions. A scree plot can be used for example to visualize this cut-off. For better understanding of intrinsic dimensionality, see the examples in Fig. 1.

Lemma 3 (Embedding from Eigenvectors of Kernel Matrix (Ghojogh et al., 2021b)). *Let $\boldsymbol{v}_k = [v_{k1}, \ldots, v_{kn}]^\top$ and δ_k be the k-th eigenvector and eigenvalue of kernel matrix, respectively. We can compute the embedding of point $\boldsymbol{x}$, denoted by $\boldsymbol{y}(\boldsymbol{x}) = [y_1(\boldsymbol{x}), \ldots, y_p(\boldsymbol{x})]^\top$ (where $p \leq n$) using the eigenvector of kernel as:*

$$y_k(\boldsymbol{x}) = \sqrt{\delta_k}\, v_{ki}. \quad (48)$$

Proof. See (Ghojogh et al., 2021b) for proof. $\square$

Another way for justifying Eq. (48) is as follows (Weinberger & Saul, 2006b). From the eigenvalue decomposition of kernel matrix, we have (Ghojogh et al., 2019a):

$$\boldsymbol{K} = \boldsymbol{V}\boldsymbol{\Delta}\boldsymbol{V}^\top$$

$$\implies \boldsymbol{K}_{ij} = \sum_{k=1}^{n} \delta_k\, v_{ki}\, v_{kj}, \quad \forall i, j \in \{1, \ldots, n\}, \quad (49)$$

where the columns of $\boldsymbol{V}$ are the eigenvectors and the diagonal elements of $\boldsymbol{\Delta}$ are eigenvalues. Also kernel can be stated as (Ghojogh et al., 2021b):

$$\boldsymbol{K}_{ij} = \phi(\boldsymbol{x}_i)^\top \phi(\boldsymbol{x}_j) \stackrel{(33)}{=} \boldsymbol{y}_i^\top \boldsymbol{y}_j. \quad (50)$$

Considering both Eqs. (49) and (50) gives:

$$\boldsymbol{y}_i^\top \boldsymbol{y}_j = \sum_{k=1}^{n} \delta_k\, v_{ki}\, v_{kj} \stackrel{(a)}{=} \sum_{k=1}^{n} \sqrt{\delta_k}\, v_{ki} \sqrt{\delta_k}\, v_{kj}$$

$$\implies \boldsymbol{y}_i(k) = \sqrt{\delta_k}\, v_{ki},$$

where $\boldsymbol{y}_i(k)$ is the k-th element of $\boldsymbol{y}_i$ and (a) is allowed because kernel matrix is positive semidefinite (see Eq. (42)) so its eigenvalues, δ_k's, are nonnegative. This equation is equal to Eq. (48).

6. Supervised Maximum Variance Unfolding

MVU is an unsupervised manifold learning method. There exist several variants for supervised MVU or supervised SDE which make use of class labels. In the following, we introduce these methods.

6.1. Supervised MVU Using kNN within Classes

One of the methods for supervised MVU or supervised SDE is (Zhang et al., 2005; Liu et al., 2005) which uses k-Nearest Neighbors (kNN) within classes. It modifies Eq. (38) in a way that the kNN graph is formed between points of every class and not amongst the entire data points. Hence, we know the k neighbors of every point in each class. Let τ_{ij} be one if $\boldsymbol{x}_i$ and $\boldsymbol{x}_i$ belong to the same class and $\boldsymbol{x}_j$ is a neighbor of $\boldsymbol{x}_i$; otherwise, it is zero. The optimization problem of MVU is the same as Eq. (47) where τ_{ij} has been computed differently.

6.2. Supervised MVU by Class-wise Unfolding

The method named SMVU1 proposed in (Wei et al., 2016) is a supervised MVU method which unfolds manifold class-wise. Let G_c denote the set of points belonging to the class c and $\bar{\boldsymbol{x}}_c$ be the mean of class c. For the class c, we define the representative $\boldsymbol{x}_c$ to be the closest point of class to the mean of class:

$$\boldsymbol{x}_c := \min_{\boldsymbol{x}_i \in G_c} \|\boldsymbol{x}_i - \bar{\boldsymbol{x}}_c\|_2^2. \quad (51)$$

Note that, rather than the above definition, one can define $\boldsymbol{x}_c$ to be the medoid of class which is the closest point to all points of the class; however, computation of medoid can be more time-consuming.

Assume we have C classes denoted by $\{c_1, \ldots, c_C\}$. Recall that local isometry yielded $\boldsymbol{K}_{ii} + \boldsymbol{K}_{jj} - 2\boldsymbol{K}_{ij} = \|\boldsymbol{x}_i - \boldsymbol{x}_j\|_2^2$. For class-wise local isometry, we can have:

$$\boldsymbol{K}_{c_i c_i} + \boldsymbol{K}_{c_j c_j} - 2\boldsymbol{K}_{c_i c_j} = \alpha^2 \|\boldsymbol{x}_{c_i} - \boldsymbol{x}_{c_j}\|_2^2, \quad (52)$$

$\forall i, j \in \{1, \ldots, C\}$, where $\alpha > 1$ is a hyperparameter (Wei et al., 2016) and $\boldsymbol{K}_{c_i c_j} := \phi(\boldsymbol{x}_{c_i})^\top \phi(\boldsymbol{x}_{c_j})$ is the kernel between representatives of classes i and j. The paper (Wei et al., 2016) considers the following pairs of classes:

$$\boldsymbol{K}_{c_i c_i} + \boldsymbol{K}_{c_{i+1} c_{i+1}} - 2\boldsymbol{K}_{c_i c_{i+1}} = \alpha^2 \|\boldsymbol{x}_{c_i} - \boldsymbol{x}_{c_j}\|_2^2,$$

$$\boldsymbol{K}_{c_i c_i} + \boldsymbol{K}_{c_C c_C} - 2\boldsymbol{K}_{c_i c_C} = \alpha^2 \|\boldsymbol{x}_{c_i} - \boldsymbol{x}_C\|_2^2,$$

$\forall i, j \in \{1, \ldots, C\}$. We define:

$$\Gamma_c = \frac{1}{2} \sum_{i=1}^{n_c} \sum_{j=1}^{n_c} (\boldsymbol{K}_{ii} + \boldsymbol{K}_{jj} - 2\boldsymbol{K}_{ij}), \forall \boldsymbol{x}_i, \boldsymbol{x}_j \in G_c, \quad (53)$$

$$\Gamma := \sum_{c=1}^{C} \frac{\Gamma_c}{n_c}. \quad (54)$$

where n_c denotes the number of points in class c. We maximize this term to maximize the variance of unfolding for each class. The SDP optimization for kernel learning is (Wei et al., 2016):

$$\underset{\boldsymbol{K}}{\text{maximize}} \quad \sum_{c=1}^{C} \frac{\Gamma_c}{n_c}$$

subject to
$$\tau_{ij}(\boldsymbol{K}_{ii} + \boldsymbol{K}_{jj} - 2\,\boldsymbol{K}_{ij}) = \tau_{ij}(\boldsymbol{G}_{ii} + \boldsymbol{G}_{jj} - 2\,\boldsymbol{G}_{ij}),$$
$$\forall i, j \in \{1, \ldots, n\},$$
$$\boldsymbol{K}_{c_i c_i} + \boldsymbol{K}_{c_{i+1} c_{i+1}} - 2\,\boldsymbol{K}_{c_i c_{i+1}} = \alpha^2 \|\boldsymbol{x}_{c_i} - \boldsymbol{x}_{c_j}\|_2^2,$$
$$\boldsymbol{K}_{c_i c_i} + \boldsymbol{K}_{c_C c_C} - 2\,\boldsymbol{K}_{c_i c_C} = \alpha^2 \|\boldsymbol{x}_{c_i} - \boldsymbol{x}_C\|_2^2,$$
$$\forall i, j \in \{1, \ldots, C\},$$
$$\sum_{i=1}^{n} \sum_{j=1}^{n} \boldsymbol{K}_{ij} = 0,$$
$$\boldsymbol{K} \succeq \boldsymbol{0},$$
(55)

where τ_{ij} is the same as defined before in Eq. (38).

6.3. Supervised MVU by Fisher Criterion

The method named SMVU2 proposed in (Wei et al., 2016) is a supervised MVU method which unfolds manifold by Fisher criterion; hence, we name this method Fisher-MVU. Fisher criterion maximizes the between-class scatter and minimizes the within-class scatter. The within-class scatter in the embedding space (or feature space equipped with kernel k) is:

$$\sigma_W := \sum_{c=1}^{C} \frac{1}{n_c} \sum_{\boldsymbol{x}_i \in G_c} \|\boldsymbol{\phi}(\boldsymbol{x}_i) - \boldsymbol{\phi}(\boldsymbol{x}_c)\|_k^2$$
$$\overset{(a)}{=} \sum_{c=1}^{C} \frac{1}{n_c} \sum_{\boldsymbol{x}_i \in G_c} (\boldsymbol{K}_{ii} + \boldsymbol{K}_{cc} - 2\boldsymbol{K}_{ci}), \quad (56)$$

where $\boldsymbol{K}_{ii} := \boldsymbol{\phi}(\boldsymbol{x}_i)^\top \boldsymbol{\phi}(\boldsymbol{x}_i)$, $\boldsymbol{K}_{cc} := \boldsymbol{\phi}(\boldsymbol{x}_c)^\top \boldsymbol{\phi}(\boldsymbol{x}_c)$, and $\boldsymbol{K}_{ci} := \boldsymbol{\phi}(\boldsymbol{x}_c)^\top \boldsymbol{\phi}(\boldsymbol{x}_i)$, and (a) is because of distance in the feature space (Schölkopf, 2001; Ghojogh et al., 2021b). The between-class scatter in the embedding space (or feature space equipped with kernel k) is:

$$\sigma_B := \sum_{c_i=1}^{C} \sum_{c_j=1}^{C} \|\boldsymbol{\phi}(\boldsymbol{x}_{c_i}) - \boldsymbol{\phi}(\boldsymbol{x}_{c_j})\|_k^2$$
$$\overset{(a)}{=} \sum_{c_i=1}^{C} \sum_{c_j=1}^{C} (\boldsymbol{K}_{c_i c_i} + \boldsymbol{K}_{c_j c_j} - 2\boldsymbol{K}_{c_i c_j}). \quad (57)$$

where (a) is because of distance in the feature space (Schölkopf, 2001; Ghojogh et al., 2021b). Note that the between-class scatter has another form which uses the mean of classes; however, as the mean of a class is not

necessarily one of the points, its embedding (in the feature space) is not available. Therefore, the scatter of all points from classes is used for computation of between-class scatter. One of the forms for Fisher criterion is (Fukunaga, 1990):

$$\Gamma = C \times (\sigma_B - \sigma_W), \quad (58)$$

which should be maximized. The SDP optimization for kernel learning is (Wei et al., 2016):

$$\underset{\boldsymbol{K}}{\text{maximize}} \quad C(\sigma_B - \sigma_W)$$
$$\text{subject to} \quad \tau_{ij}(\boldsymbol{K}_{ii} + \boldsymbol{K}_{jj} - 2\,\boldsymbol{K}_{ij})$$
$$= \tau_{ij}(\boldsymbol{G}_{ii} + \boldsymbol{G}_{jj} - 2\,\boldsymbol{G}_{ij}),$$
$$\forall i, j \in \{1, \ldots, n\}, \quad (59)$$
$$\sum_{i=1}^{n} \sum_{j=1}^{n} \boldsymbol{K}_{ij} = 0,$$
$$\boldsymbol{K} \succeq \boldsymbol{0}.$$

6.4. Supervised MVU by Colored MVU

One of the supervised approches for MVU is colored MVU (Song et al., 2007) which uses some side information such as labels. In its formulation, it uses the Hilbert-Schmidt Independence Criterion (HSIC) (Gretton et al., 2005) between embedded data points $\{\boldsymbol{y}_i = \boldsymbol{\phi}(\boldsymbol{x}_i)\}_{i=1}^{n}$ and labels $\{l_i\}_{i=1}^{n}$:

$$\text{HSIC} := \frac{1}{(n-1)^2} \mathbf{tr}(\boldsymbol{K}_l \boldsymbol{H} \boldsymbol{K} \boldsymbol{H})$$
$$\overset{(a)}{=} \frac{1}{(n-1)^2} \mathbf{tr}(\boldsymbol{H} \boldsymbol{K} \boldsymbol{H} \boldsymbol{K}_l), \quad (60)$$

where (a) is because of cyclic property of trace, $\boldsymbol{K} \in \mathbb{R}^{n \times n}$ and $\boldsymbol{K}_l \in \mathbb{R}^{n \times n}$ are kernel matrices over embedded points and labels, respectively, and $\mathbb{R}^{n \times n} \ni \boldsymbol{H} := \boldsymbol{I} - (1/n)\boldsymbol{1}\boldsymbol{1}^\top$ is the centering matrix. HSIC is a measure of dependence between two random variables (Ghojogh et al., 2021b). Colored MVU maximizes the HSIC between the embedded points and the labels; in other words, the dependence of embedding and labels is maximized to be supervised. Therefore, colored MVU maximizes Eq. (60), i.e. $\mathbf{tr}(\boldsymbol{H} \boldsymbol{K} \boldsymbol{H} \boldsymbol{K}_l)$ or $\mathbf{tr}(\boldsymbol{K} \boldsymbol{H} \boldsymbol{K}_l \boldsymbol{H})$, rather than maximizing $\mathbf{tr}(\boldsymbol{K})$ which is done in MVU (Song et al., 2007):

$$\underset{\boldsymbol{K}}{\text{maximize}} \quad \mathbf{tr}(\boldsymbol{H} \boldsymbol{K} \boldsymbol{H} \boldsymbol{K}_l)$$
$$\text{subject to} \quad \tau_{ij}(\boldsymbol{K}_{ii} + \boldsymbol{K}_{jj} - 2\,\boldsymbol{K}_{ij})$$
$$= \tau_{ij}(\boldsymbol{G}_{ii} + \boldsymbol{G}_{jj} - 2\,\boldsymbol{G}_{ij}),$$
$$\forall i, j \in \{1, \ldots, n\}, \quad (61)$$
$$\sum_{i=1}^{n} \sum_{j=1}^{n} \boldsymbol{K}_{ij} = 0,$$
$$\boldsymbol{K} \succeq \boldsymbol{0}.$$

Note that as kernel is a soft measure of similarity (Ghojogh et al., 2021b), the labels or side information $\{l_i\}_{i=1}^n$ can be soft labels (e.g., regression labels) or hard labels (e.g., classification labels). In case of hard labels, one of the best choices for the $\boldsymbol{K}_l$ is delta kernel (Barshan et al., 2011) where the (i, j)-th element of kernel is:

$$\boldsymbol{K}_l(i, j) = \delta_{\boldsymbol{l}_i, \boldsymbol{l}_j} := \begin{cases} 1 & \text{if } \boldsymbol{l}_i = \boldsymbol{l}_j, \\ 0 & \text{if } \boldsymbol{l}_i \neq \boldsymbol{l}_j, \end{cases} \quad (62)$$

where $\delta_{\boldsymbol{l}_i, \boldsymbol{l}_j}$ is the Kronecker delta which is one if the $\boldsymbol{x}_i$ and $\boldsymbol{x}_j$ belong to the same class.

7. Out-of-sample Extension of MVU

There are several approaches for out-of-sample extension of MVU. In the following, we introduce some of these approaches which are approaches using eigenfunctions (Chin & Suter, 2008) and kernel mapping (Gisbrecht et al., 2015). There exist some other methods for out-of-sample extension such as (Bunte et al., 2012) which we do not cover here.

7.1. Out-of-sample Extension Using Eigenfunctions

One of the methods for out-of-sample extension of MVU is using eigenfunctions (Chin & Suter, 2008). Recall Eq. (5) which relates the eigenvectors of kernel function and eigenfunctions of kernel operator. According to (Schwaighofer et al., 2005), this equation can be slightly modified to:

$$f_k(\boldsymbol{x}) = \sum_{i=1}^n b_{ki}\, r(\boldsymbol{x}_i, \boldsymbol{x}) = \sum_{i=1}^n b_{ki}\, r(\boldsymbol{x}, \boldsymbol{x}_i), \quad (63)$$

where $r(., .)$ is an auxiliary smoothing kernel such as the RBF kernel, and b_{ki} is the i-th element of:

$$\mathbb{R}^n \ni \boldsymbol{b}_k := (\boldsymbol{R} + \eta \boldsymbol{I})^{-1} \boldsymbol{v}_k, \quad (64)$$

where $\boldsymbol{v}_k$ is the k-th eigenvector of kernel matrix $\boldsymbol{K} \in \mathbb{R}^{n \times n}$ over training data, and $\boldsymbol{R} \in \mathbb{R}^{n \times n}$ is the smoothing kernel matrix on the n training data points using kernel $r(., .)$ and $\eta > 0$ is a regularization parameter for stable inverse of matrix.

According to the Mercer's theorem (Ghojogh et al., 2021b), the kernel can be written as (Chin & Suter, 2008):

$$k(\boldsymbol{x}, \boldsymbol{x}_i) = \sum_{j=1}^n \lambda_j \psi_j(\boldsymbol{x}) \psi_j(\boldsymbol{x}_i)$$
$$\overset{(a)}{=} r(\boldsymbol{x})^\top (\boldsymbol{R} + \eta \boldsymbol{I})^{-1} \boldsymbol{K} (\boldsymbol{R} + \eta \boldsymbol{I})^{-1} r(\boldsymbol{x}_i) \quad (65)$$

where (a) is because of Eqs. (63) and (64), $r(\boldsymbol{x}) := [r(\boldsymbol{x}_1, \boldsymbol{x}), \dots, r(\boldsymbol{x}_n, \boldsymbol{x})]^\top \in \mathbb{R}^n$, $\{\psi_j\}_{j=1}^n$ and $\{\lambda_j\}_{j=1}^n$ are the eigenfunctions and eigenvalues of the kernel operator k, respectively. According to Eq. (7), we have:

$$y_k(\boldsymbol{x}) = \frac{1}{\sqrt{\delta_k}} \sum_{i=1}^n v_{ki}\, k(\boldsymbol{x}, \boldsymbol{x}_i) \overset{(65)}{=} \boldsymbol{p}_k\, r(\boldsymbol{x}), \quad (66)$$

where δ_k is the k-th eigenvalue of kernel matrix $\boldsymbol{K}$ and (Chin & Suter, 2008):

$$\mathbb{R}^{1 \times n} \ni \boldsymbol{p}_k := \delta_k^{-1/2} \boldsymbol{v}_k^\top \boldsymbol{R} (\boldsymbol{R} + \eta \boldsymbol{I})^{-1} \boldsymbol{K} (\boldsymbol{R} + \eta \boldsymbol{I})^{-1}. \quad (67)$$

Therefore, for a point $\boldsymbol{x}$ which can be an out-of-sample point, the k-th dimension of embedding is calculated using Eq. (66) and considering the top $p \leq n$ dimensions of embedding gives $\mathbb{R}^p \ni \boldsymbol{y}(\boldsymbol{x}) = [y_1(\boldsymbol{x}), \dots, y_p(\boldsymbol{x})]^\top$.

7.2. Out-of-sample Extension Using Kernel Mapping

There is a kernel mapping method (Gisbrecht et al., 2015) to embed the out-of-sample data in MVU. We introduce this method here. We define a map which maps any data point as $\boldsymbol{x} \mapsto \boldsymbol{y}(\boldsymbol{x})$, where:

$$\mathbb{R}^p \ni \boldsymbol{y}(\boldsymbol{x}) := \sum_{j=1}^n \boldsymbol{\alpha}_j \frac{k(\boldsymbol{x}, \boldsymbol{x}_j)}{\sum_{\ell=1}^n k(\boldsymbol{x}, \boldsymbol{x}_\ell)}, \quad (68)$$

and $\boldsymbol{\alpha}_j \in \mathbb{R}^p$, and $\boldsymbol{x}_j$ and $\boldsymbol{x}_\ell$ denote the j-th and ℓ-th training data points, respectively. The $k(\boldsymbol{x}, \boldsymbol{x}_j)$ is a kernel such as the Gaussian kernel:

$$k(\boldsymbol{x}, \boldsymbol{x}_j) = \exp\left(\frac{-||\boldsymbol{x} - \boldsymbol{x}_j||_2^2}{2\,\sigma_j^2}\right), \quad (69)$$

where σ_j is calculated as (Gisbrecht et al., 2015):

$$\sigma_j := \gamma \times \min_i(||\boldsymbol{x}_j - \boldsymbol{x}_i||_2), \quad (70)$$

where γ is a small positive number.

Assume we have already embedded the training data points using MVU; therefore, the set $\{\boldsymbol{y}_i\}_{i=1}^n$ is available. If we map the training data points, we want to minimize the following least-squares cost function in order to get $\boldsymbol{y}(\boldsymbol{x}_i)$ close to $\boldsymbol{y}_i$ for the i-th training point:

$$\underset{\boldsymbol{\alpha}_j\text{'s}}{\text{minimize}} \quad \sum_{i=1}^n ||\boldsymbol{y}_i - \boldsymbol{y}(\boldsymbol{x}_i)||_2^2, \quad (71)$$

where the summation is over the training data points. We can write this cost function in matrix form as below:

$$\underset{\boldsymbol{A}}{\text{minimize}} \quad ||\boldsymbol{Y} - \boldsymbol{K}'' \boldsymbol{A}||_F^2, \quad (72)$$

where $\mathbb{R}^{n \times p} \ni \boldsymbol{Y} := [\boldsymbol{y}_1, \dots, \boldsymbol{y}_n]^\top$ and $\mathbb{R}^{n \times p} \ni \boldsymbol{A} := [\boldsymbol{\alpha}_1, \dots, \boldsymbol{\alpha}_n]^\top$. The $\boldsymbol{K}'' \in \mathbb{R}^{n \times n}$ is the kernel matrix whose (i, j)-th element is defined to be:

$$\boldsymbol{K}''(i, j) := \frac{k(\boldsymbol{x}_i, \boldsymbol{x}_j)}{\sum_{\ell=1}^n k(\boldsymbol{x}_i, \boldsymbol{x}_\ell)}. \quad (73)$$

The Eq. (72) is always non-negative; thus, its smallest value is zero. Therefore, the solution to this equation is:

$$\boldsymbol{Y} - \boldsymbol{K}'' \boldsymbol{A} = \boldsymbol{0} \implies \boldsymbol{Y} = \boldsymbol{K}'' \boldsymbol{A}$$
$$\overset{(a)}{\implies} \boldsymbol{A} = \boldsymbol{K}''^\dagger \boldsymbol{Y}, \quad (74)$$

where $\boldsymbol{K}''^{\dagger}$ is the pseudo-inverse of $\boldsymbol{K}''$:

$$\boldsymbol{K}''^{\dagger} = (\boldsymbol{K}''^{\top} \boldsymbol{K}'')^{-1} \boldsymbol{K}''^{\top}, \qquad (75)$$

and (a) is because $\boldsymbol{K}''^{\dagger} \boldsymbol{K}'' = \boldsymbol{I}$.

Finally, the mapping of Eq. (68) for the n_t out-of-sample data points is:

$$\boldsymbol{Y}_t = \boldsymbol{K}''_t \boldsymbol{A}, \qquad (76)$$

where the (i, j)-th element of the out-of-sample kernel matrix $\boldsymbol{K}''_t \in \mathbb{R}^{n_t \times n}$ is:

$$\boldsymbol{K}''_t(i, j) := \frac{k(\boldsymbol{x}_i^{(t)}, \boldsymbol{x}_j)}{\sum_{\ell=1}^{n} k(\boldsymbol{x}_i^{(t)}, \boldsymbol{x}_\ell)}, \qquad (77)$$

where $\boldsymbol{x}_i^{(t)}$ is the i-th out-of-sample data point, and $\boldsymbol{x}_j$ and $\boldsymbol{x}_\ell$ are the j-th and ℓ-th training data points.

8. Other Variants of Maximum Variance Unfolding

8.1. Action Respecting Embedding

Most of dimensionality reduction methods, including MVU, do not care about the order of points. However, some data may consist of temporal information; for example, the frames of a video where the order of images matters. In this case, a variant of MVU is required which considers the temporal information when unfolding the manifold of data. Action Respecting Embedding (ARE) (Bowling et al., 2005) is an MVU variant caring about order of points. It has various applications in reinforcement learning and robotics (Bowling et al., 2007). ARE has the same constraints in the optimization of MVU plus one additional constraint about temporal information. Assume two actions (e.g., rotation or transformation of image or a combination of rotation and transformation), denoted by a_i and a_j, are applied on data points $\boldsymbol{x}_i$ and $\boldsymbol{x}_j$ to result in $\boldsymbol{x}_{i+1}$ and $\boldsymbol{x}_{j+1}$, respectively:

$$\boldsymbol{x}_i \xrightarrow{a_i} \boldsymbol{x}_{i+1},$$
$$\boldsymbol{x}_j \xrightarrow{a_j} \boldsymbol{x}_{j+1}.$$

Consider the same actions in the embedding space of MVU, i.e. the feature space:

$$\boldsymbol{\phi}(\boldsymbol{x}_i) \xrightarrow{a_i} \boldsymbol{\phi}(\boldsymbol{x}_{i+1}),$$
$$\boldsymbol{\phi}(\boldsymbol{x}_j) \xrightarrow{a_j} \boldsymbol{\phi}(\boldsymbol{x}_{j+1}).$$

If the two actions a_i and a_j are equal, the distances of embedded points should remain the same before and after the action:

$$a_i = a_j \implies \|\boldsymbol{\phi}(\boldsymbol{x}_i) - \boldsymbol{\phi}(\boldsymbol{x}_j)\|_k^2$$
$$= \|\boldsymbol{\phi}(\boldsymbol{x}_{i+1}) - \boldsymbol{\phi}(\boldsymbol{x}_{j+1})\|_k^2$$
$$\overset{(a)}{\implies} \boldsymbol{K}_{ii} + \boldsymbol{K}_{jj} - 2\boldsymbol{K}_{ij}$$
$$= \boldsymbol{K}_{i+1,i+1} + \boldsymbol{K}_{j+1,j+1} - 2\boldsymbol{K}_{i+1,j+1}, \quad (78)$$
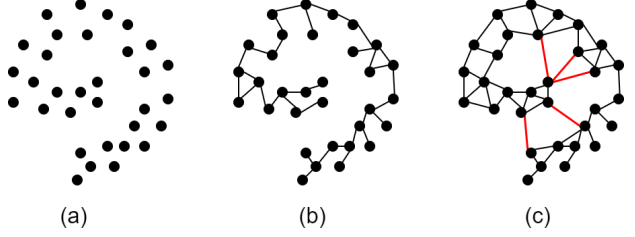

(a) (b) (c)

Figure 3. Visualizing the possible problem of short circuit: (a) data points lying on a Swiss roll manifold, (b) Correct kNN graph for the manifold, (c) and incorrect kNN graph having short circuits (shown by red edges) by some larger value for k.

where (a) is because of distance in the feature space (Schölkopf, 2001; Ghojogh et al., 2021b). Finally, given actions $\{a_i\}_{i=1}^n$, the optimization in ARE is:

$$\underset{\boldsymbol{K}}{\text{maximize}} \quad \mathbf{tr}(\boldsymbol{K})$$

subject to

$$\boldsymbol{K}_{ii} + \boldsymbol{K}_{jj} - 2\boldsymbol{K}_{ij} = \boldsymbol{G}_{ii} + \boldsymbol{G}_{jj} - 2\boldsymbol{G}_{ij},$$
$$\forall i, j \in \{1, \dots, n\},$$
$$\boldsymbol{K}_{ii} + \boldsymbol{K}_{jj} - 2\boldsymbol{K}_{ij} = \boldsymbol{K}_{i+1,i+1} + \boldsymbol{K}_{j+1,j+1} - 2\boldsymbol{K}_{i+1,j+1},$$
$$\forall i, j : a_i = a_j,$$
$$\sum_{i=1}^{n} \sum_{j=1}^{n} \boldsymbol{K}_{ij} = 0,$$
$$\boldsymbol{K} \succeq \boldsymbol{0},$$

$$(79)$$

which is a SDP problem. The solution of this problem gives a kernel for unfolding the manifold of data where the temporal information of actions is taken into account. After finding the kernel from optimization, the unfolded embedding is calculated by Eq. (48).

8.2. Relaxed Maximum Variance Unfolding

Two problems exist in MVU which are addressed in relaxed MVU (Hou et al., 2008). In the following, we explain these problems and how relaxed MVU resolves them.

8.2.1. SHORT CIRCUITS IN kNN GRAPH

For some k values, some short circuits may happen in kNN graph. For example, see Fig. 3. These short circuits result in incorrect unfolding of manifold. Let kNN$(\boldsymbol{x}_i)$ denote the set of k nearest neighbor points of $\boldsymbol{x}_i$. Consider a kNN of data where $v(i, j)$ is an edge between $\boldsymbol{x}_i$ and $\boldsymbol{x}_j$ in this graph. We define the deviation of an edge $v(i, j)$ as (Hou et al., 2008):

$$d(v(i, j)) := \frac{1}{|k\text{NN}(\boldsymbol{x}_i) \cup k\text{NN}(\boldsymbol{x}_j)|} \times \sum_{\boldsymbol{x}_l \in k\text{NN}(\boldsymbol{x}_i) \cup k\text{NN}(\boldsymbol{x}_j)} \|\boldsymbol{x}_l - \boldsymbol{x}_{ij}^{(\text{mid})}\|_2^2, \quad (80)$$

where $\boldsymbol{x}_{ij}^{(\text{mid})} := (\boldsymbol{x}_i + \boldsymbol{x}_j)/2$ and $|.|$ is the size of set. This deviation is related to the density of points; that is, the lower the density, the larger the deviation. We sort the deviation of points from smallest to largest and can discard the points from kNN which are larger than a threshold. A scree plot can be used for finding the suitable threshold.

8.2.2. RESCALING LOCAL DISTANCES

In some cases, the mapping is conformal but not isometric. Conformal maps are locally isometric but up to a scale. Let $s(\boldsymbol{x}_i)$ denote the average distance of $\boldsymbol{x}_i$ to its k nearest neighbors. Assuming that the original sampling in the input space is uniform, the conformal scaling factor between points $\boldsymbol{x}_i$ and $\boldsymbol{x}_j$ is $(s(\boldsymbol{x}_i)s(\boldsymbol{x}_j))^{1/2}$ (De Silva & Tenenbaum, 2003). Relaxed MVU shows to be robust to violation of this assumption (Hou et al., 2008). Relaxed MVU scales the distances of points in the local isometry constraint:

$$\tau_{ij}(\boldsymbol{K}_{ii} + \boldsymbol{K}_{jj} - 2\,\boldsymbol{K}_{ij})$$
$$= \tau_{ij}\|(s(\boldsymbol{x}_i)s(\boldsymbol{x}_j))^{1/2}(\boldsymbol{x}_i - \boldsymbol{x}_j)\|_2^2. \tag{81}$$

8.3. Landmark Maximum Variance Unfolding for Big Data

As explained in Section 3, MVU uses interior-point method which is slow especially for big data. Landmark SDE or Landmark MVU (Weinberger et al., 2005) uses randomly selected landmarks from data points. Let n and $m \ll n$ denote the total number of points and the number of landmarks, respectively, and $\{\boldsymbol{\mu}_\alpha\}_{\alpha=1}^m \subset \{\boldsymbol{x}_i\}_{i=1}^n$ be the landmarks. Every point can be reconstructed linearly by the landmarks:

$$\widehat{\boldsymbol{x}}_i = \sum_{\alpha=1}^m q_{i\alpha}\,\boldsymbol{\mu}_\alpha, \tag{82}$$

where $q_{i\alpha}, \forall i, \alpha$ are the reconstruction weights. Inspired by Locally Linear embedding (LLE) (Ghojogh et al., 2020a), every embedded point should also be reconstructed from the embedded landmarks, denoted by $\{\boldsymbol{\ell}_\alpha\}_{\alpha=1}^m = \{\boldsymbol{\phi}(\boldsymbol{\mu}_\alpha)\}_{\alpha=1}^m$, with the same reconstruction weights:

$$\widehat{\boldsymbol{y}}_i = \sum_{\alpha=1}^m q_{i\alpha}\,\boldsymbol{\ell}_\alpha. \tag{83}$$

Kernel can be stated as inner product of points in the feature space (Ghojogh et al., 2021b):

$$\boldsymbol{K}_{ij} = \boldsymbol{\phi}(\boldsymbol{x}_i)^\top \boldsymbol{\phi}(\boldsymbol{x}_j) \overset{(33)}{=} \boldsymbol{y}_i^\top \boldsymbol{y}_j \implies \boldsymbol{K}_{ij} \approx \widehat{\boldsymbol{y}}_i^\top \widehat{\boldsymbol{y}}_j.$$
$$\overset{(83)}{\implies} \boldsymbol{K}_{ij} \approx q_{i\alpha}\boldsymbol{\ell}_\alpha^\top \boldsymbol{\ell}_\beta q_{i\beta} \implies \boldsymbol{K} = \boldsymbol{V}\boldsymbol{L}\boldsymbol{V}^\top, \tag{84}$$

where $\boldsymbol{Q}_{i\alpha} = q_{i\alpha}$, $\boldsymbol{Q} \in \mathbb{R}^{n\times m}$, and $\boldsymbol{L} = \boldsymbol{\ell}_\alpha^\top \boldsymbol{\ell}_\beta \in \mathbb{R}^{m\times m}$. This decomposition of $\boldsymbol{L}$ shows that $\boldsymbol{L} \succeq \boldsymbol{0}$ which will be used as one of the constraints in optimization. Now,

consider linear reconstruction of points by all points in the training set:

$$\min_{w_{ij}} \quad \sum_{i=1}^n \|\boldsymbol{x}_i - \sum_{j=1}^n w_{ij}\boldsymbol{x}_j\|_2^2, \tag{85}$$

where w_{ij}'s are the reconstruction weights. This optimization also exists in LLE and can be restated as (Ghojogh et al., 2020a):

$$\min_{\boldsymbol{M}} \quad \sum_{i=1}^n \sum_{j=1}^n \boldsymbol{M}_{ij}\boldsymbol{x}_i\boldsymbol{x}_j, \tag{86}$$

where $\mathbb{R}^{n\times n} \ni \boldsymbol{M} := (\boldsymbol{I} - \boldsymbol{W})^\top(\boldsymbol{I} - \boldsymbol{W})$ where $\boldsymbol{W}_{ij} = w_{ij}$. The matrix $\boldsymbol{M}$ can be found by solving the least squares problem in Eq. (86). Considering the $m \ll n$ landmarks, we can decompose the matrix $\boldsymbol{M}$ as:

$$\boldsymbol{M} \approx \left[\begin{array}{c|c} \boldsymbol{M}^{ll} \in \mathbb{R}^{m\times m} & \boldsymbol{M}^{lu} \in \mathbb{R}^{m\times(n-m)} \\ \hline \boldsymbol{M}^{ul} \in \mathbb{R}^{(n-m)\times m} & \boldsymbol{M}^{uu} \in \mathbb{R}^{(n-m)\times(n-m)} \end{array} \right]. \tag{87}$$

As the reconstruction weights $q_{i\alpha}, \forall i, \alpha$ can be seen as a subset of reconstruction weights w_{ij}, we can write $\boldsymbol{Q}$ using the parts of matrix $\boldsymbol{M}$ (Weinberger et al., 2005):

$$\mathbb{R}^{n\times m} \ni \boldsymbol{Q} = \left[\begin{array}{c} \boldsymbol{I}_{m\times m} \\ (\boldsymbol{M}^{uu})^{-1}\boldsymbol{M}^{ul} \end{array} \right]. \tag{88}$$

Note that this usage of a small part of matrix (because $m \ll n$) is inspired by the Nyström method (Ghojogh et al., 2021b).

Landmark MVU solves the following SDP optimization problem (Weinberger et al., 2005):

$$\begin{aligned} \underset{\boldsymbol{L}}{\text{maximize}} \quad & \mathbf{tr}(\boldsymbol{Q}\boldsymbol{L}\boldsymbol{Q}^\top) \\ \text{subject to} \quad & \tau_{ij}((\boldsymbol{Q}\boldsymbol{L}\boldsymbol{Q}^\top)_{ii} + (\boldsymbol{Q}\boldsymbol{L}\boldsymbol{Q}^\top)_{jj} - 2\,(\boldsymbol{Q}\boldsymbol{L}\boldsymbol{Q}^\top)_{ij}) \\ & \qquad \leq \tau_{ij}(\boldsymbol{G}_{ii} + \boldsymbol{G}_{jj} - 2\,\boldsymbol{G}_{ij}), \\ & \qquad\qquad \forall i, j \in \{1, \dots, n\}, \\ & \sum_{i=1}^n \sum_{j=1}^n (\boldsymbol{Q}\boldsymbol{L}\boldsymbol{Q}^\top)_{ij} = 0, \\ & \boldsymbol{L} \succeq \boldsymbol{0}, \end{aligned} \tag{89}$$

where the optimization variable is the small matrix $\boldsymbol{L} \in \mathbb{R}^{m\times m}$ rather than the large matrix $\boldsymbol{K} \in \mathbb{R}^{n\times n}$; hence, a big problem is reduced to an efficient small one. Note that the paper (Weinberger et al., 2005) has converted the equality of local isometry constraint to inequality. This is okay because it has made the constraint more restricted and harder than the equality constraint. After solving the optimization problem to find the optimal $\boldsymbol{L}$, we use Eqs. (88) and (84) to calculate $\boldsymbol{K}$ and then embedding is calculated using Eq. (48).

8.4. Other Improvements over Maximum Variance Unfolding and Kernel Learning

An existing book chapter on MVU is (Wang, 2012, Chapter 9). There have been other improvements over MVU. There exist some other improvements over MVU and kernel learning by SDP whose details we do not cover in this paper. We list these improvements here. An application of MVU in nonlinear process monitoring can be found in (Liu et al., 2014). SDP has also been used for kernel matrix completion (Graepel, 2002) and low-rank kernel learning (Kulis et al., 2006). Maximum covariance unfolding (Mahadevan et al., 2011) has been proposed for bimodal manifold unfolding. We can also interpret MVU as a regularized shortest path problem on the graph of data (Paprotny & Garcke, 2012); hence, it can be related to the Isomap algorithm (Ghojogh et al., 2020b).

9. Conclusion

In this paper, we first explained how the spectral dimensionality reduction methods can be unified as kernel PCA with different kernels using eigenfunction learning and kernel construction by distance matrices. Then, we said as the spectral methods are unified as kernel PCA, let us learn the best kernel for unfolding the manifold of data. We introduced MVU and its variants as some methods for learning the best kernel for manifold unfolding using SDP optimization problems.

Acknowledgement

References

Alipanahi, Babak and Ghodsi, Ali. Guided locally linear embedding. *Pattern recognition letters*, 32(7):1029–1035, 2011.

Barshan, Elnaz, Ghodsi, Ali, Azimifar, Zohreh, and Jahromi, Mansoor Zolghadri. Supervised principal component analysis: Visualization, classification and regression on subspaces and submanifolds. *Pattern Recognition*, 44(7):1357–1371, 2011.

Belkin, Mikhail and Niyogi, Partha. Laplacian eigenmaps and spectral techniques for embedding and clustering. In *Nips*, volume 14, pp. 585–591, 2001.

Bengio, Yoshua, Paiement, Jean-fran␣çcois, Vincent, Pascal, Delalleau, Olivier, Roux, Nicolas, and Ouimet, Marie. Out-of-sample extensions for LLE, Isomap, MDS, eigenmaps, and spectral clustering. *Advances in neural information processing systems*, 16:177–184, 2003a.

Bengio, Yoshua, Vincent, Pascal, Paiement, Jean-François, Delalleau, O, Ouimet, M, and LeRoux, N. Learning eigenfunctions of similarity: linking spectral clustering and kernel PCA. Technical report, Departement d'Informatique et Recherche Operationnelle, 2003b.

Bengio, Yoshua, Vincent, Pascal, Paiement, Jean-François, Delalleau, Olivier, Ouimet, Marie, and Le Roux, Nicolas. Spectral clustering and kernel PCA are learning eigenfunctions. Technical report, Departement d'Informatique et Recherche Operationnelle, Technical Report 1239, 2003c.

Bengio, Yoshua, Delalleau, Olivier, Roux, Nicolas Le, Paiement, Jean-François, Vincent, Pascal, and Ouimet, Marie. Learning eigenfunctions links spectral embedding and kernel PCA. *Neural computation*, 16(10): 2197–2219, 2004.

Bengio, Yoshua, Delalleau, Olivier, Le Roux, Nicolas, Paiement, Jean-François, Vincent, Pascal, and Ouimet, Marie. Spectral dimensionality reduction. In *Feature Extraction*, pp. 519–550. Springer, 2006.

Bowling, Michael, Ghodsi, Ali, and Wilkinson, Dana. Action respecting embedding. In *Proceedings of the 22nd international conference on Machine learning*, pp. 65–72, 2005.

Bowling, Michael, Wilkinson, Dana, Ghodsi, Ali, and Milstein, Adam. Subjective localization with action respecting embedding. In *Robotics Research*, pp. 190–202. Springer, 2007.

Boyd, Stephen, Boyd, Stephen P, and Vandenberghe, Lieven. *Convex optimization*. Cambridge university press, 2004.

Bunte, Kerstin, Biehl, Michael, and Hammer, Barbara. A general framework for dimensionality-reducing data visualization mapping. *Neural Computation*, 24(3):771–804, 2012.

Chin, Tat-Jun and Suter, David. Out-of-sample extrapolation of learned manifolds. *IEEE Transactions on Pattern Analysis and Machine Intelligence*, 30(9):1547–1556, 2008.

Coifman, Ronald R and Lafon, Stéphane. Diffusion maps. *Applied and computational harmonic analysis*, 21(1):5–30, 2006.

Cox, Michael AA and Cox, Trevor F. Multidimensional scaling. In *Handbook of data visualization*, pp. 315–347. Springer, 2008.

De Silva, Vin and Tenenbaum, Joshua B. Global versus local methods in nonlinear dimensionality reduction. *Advances in neural information processing systems*, pp. 721–728, 2003.

Fukunaga, Keinosuke. *Introduction to statistical pattern recognition*. Academic Press, 1990.

Ghojogh, Benyamin. *Data Reduction Algorithms in Machine Learning and Data Science*. PhD thesis, University of Waterloo, 2021.

Ghojogh, Benyamin and Crowley, Mark. Unsupervised and supervised principal component analysis: Tutorial. *arXiv preprint arXiv:1906.03148*, 2019.

Ghojogh, Benyamin, Karray, Fakhri, and Crowley, Mark. Eigenvalue and generalized eigenvalue problems: Tutorial. *arXiv preprint arXiv:1903.11240*, 2019a.

Ghojogh, Benyamin, Samad, Maria N, Mashhadi, Sayema Asif, Kapoor, Tania, Ali, Wahab, Karray, Fakhri, and Crowley, Mark. Feature selection and feature extraction in pattern analysis: A literature review. *arXiv preprint arXiv:1905.02845*, 2019b.

Ghojogh, Benyamin, Ghodsi, Ali, Karray, Fakhri, and Crowley, Mark. Locally linear embedding and its variants: Tutorial and survey. *arXiv preprint arXiv:2011.10925*, 2020a.

Ghojogh, Benyamin, Ghodsi, Ali, Karray, Fakhri, and Crowley, Mark. Multidimensional scaling, Sammon mapping, and Isomap: Tutorial and survey. *arXiv preprint arXiv:2009.08136*, 2020b.

Ghojogh, Benyamin, Ghodsi, Ali, Karray, Fakhri, and Crowley, Mark. Laplacian-based dimensionality reduction including spectral clustering, Laplacian eigenmap, locality preserving projection, graph embedding, and diffusion map: Tutorial and survey. *arXiv preprint arXiv:2106.02154*, 2021a.

Ghojogh, Benyamin, Karray, Fakhri, and Crowley, Mark. Reproducing kernel Hilbert space, Mercer's theorem, eigenfunctions, Nyström method, and use of kernels in machine learning: Tutorial and survey. *arXiv preprint arXiv:2106.08443*, 2021b.

Gisbrecht, Andrej, Schulz, Alexander, and Hammer, Barbara. Parametric nonlinear dimensionality reduction using kernel t-sne. *Neurocomputing*, 147:71–82, 2015.

Graepel, Thore. Kernel matrix completion by semidefinite programming. In *International Conference on Artificial Neural Networks*, pp. 694–699. Springer, 2002.

Grant, Michael, Boyd, Stephen, and Ye, Yinyu. CVX: Matlab software for disciplined convex programming, 2008.

Gretton, Arthur, Bousquet, Olivier, Smola, Alex, and Schölkopf, Bernhard. Measuring statistical dependence with Hilbert-Schmidt norms. In *International conference on algorithmic learning theory*, pp. 63–77. Springer, 2005.

Ham, Jihun, Lee, Daniel D, Mika, Sebastian, and Schölkopf, Bernhard. A kernel view of the dimensionality reduction of manifolds. In *Proceedings of the twenty-first international conference on Machine learning*, pp. 47, 2004.

Hou, Chenping, Jiao, Yuanyuan, Wu, Yi, and Yi, Dongyun. Relaxed maximum-variance unfolding. *Optical Engineering*, 47(7):077202, 2008.

Karimi, Amir-Hossein. A summary of the kernel matrix, and how to learn it effectively using semidefinite programming. *arXiv preprint arXiv:1709.06557*, 2017.

Kulis, Brian, Sustik, Mátyás, and Dhillon, Inderjit. Learning low-rank kernel matrices. In *Proceedings of the 23rd international conference on Machine learning*, pp. 505–512, 2006.

Lanckriet, Gert RG, Cristianini, Nello, Bartlett, Peter, Ghaoui, Laurent El, and Jordan, Michael I. Learning the kernel matrix with semidefinite programming. *Journal of Machine learning research*, 5(Jan):27–72, 2004.

Liu, Ning, Bai, Fengshan, Yan, Jun, Zhang, Benyu, Chen, Zheng, and Ma, Wei-Ying. Supervised semi-definite embedding for email data cleaning and visualization. In *Asia-Pacific Web Conference*, pp. 972–982. Springer, 2005.

Liu, Yuan-Jui, Chen, Tao, and Yao, Yuan. Nonlinear process monitoring and fault isolation using extended maximum variance unfolding. *Journal of process control*, 24 (6):880–891, 2014.

Mahadevan, Vijay, Wong, Chi, Pereira, Jose, Liu, Tom, Vasconcelos, Nuno, and Saul, Lawrence. Maximum covariance unfolding: Manifold learning for bimodal data. *Advances in Neural Information Processing Systems*, 24: 918–926, 2011.

Nesterov, Yurii and Nemirovskii, Arkadii. *Interior-point polynomial algorithms in convex programming*. SIAM, 1994.

Ng, Andrew, Jordan, Michael, and Weiss, Yair. On spectral clustering: Analysis and an algorithm. *Advances in neural information processing systems*, 14:849–856, 2001.

Paprotny, Alexander and Garcke, Jochen. On a connection between maximum variance unfolding, shortest path problems and Isomap. In *Artificial Intelligence and Statistics*, pp. 859–867. PMLR, 2012.

Roweis, Sam T and Saul, Lawrence K. Nonlinear dimensionality reduction by locally linear embedding. *Science*, 290(5500):2323–2326, 2000.

Saul, Lawrence K and Roweis, Sam T. Think globally, fit locally: unsupervised learning of low dimensional manifolds. *Journal of Machine Learning Research*, 4:119–155, 2003.

Schölkopf, Bernhard. The kernel trick for distances. *Advances in neural information processing systems*, pp. 301–307, 2001.

Schölkopf, Bernhard, Smola, Alexander J, and Bach, Francis. *Learning with kernels: support vector machines, regularization, optimization, and beyond*. MIT press, 2002.

Schwaighofer, Anton, Tresp, Volker, and Yu, Kai. Learning gaussian process kernels via hierarchical bayes. In *Advances in neural information processing systems*, pp. 1209–1216, 2005.

Song, Le, Smola, Alexander J, Borgwardt, Karsten M, Gretton, Arthur, et al. Colored maximum variance unfolding. In *Nips*, pp. 1385–1392. Citeseer, 2007.

Stewart, Gilbert W. On the early history of the singular value decomposition. *SIAM review*, 35(4):551–566, 1993.

Strange, Harry and Zwiggelaar, Reyer. *Open Problems in Spectral Dimensionality Reduction*. Springer, 2014.

Tenenbaum, Joshua B, De Silva, Vin, and Langford, John C. A global geometric framework for nonlinear dimensionality reduction. *Science*, 290(5500):2319–2323, 2000.

Vandenberghe, Lieven and Boyd, Stephen. Semidefinite programming. *SIAM review*, 38(1):49–95, 1996.

Vapnik, Vladimir. *The nature of statistical learning theory*. Springer science & business media, 1995.

Wang, Jianzhong. *Geometric structure of high-dimensional data and dimensionality reduction*, volume 5. Springer, 2012.

Wei, Chihang, Chen, Junghui, and Song, Zhihuan. Developments of two supervised maximum variance unfolding algorithms for process classification. *Chemometrics and Intelligent Laboratory Systems*, 159:31–44, 2016.

Weinberger, Kilian Q and Saul, Lawrence K. An introduction to nonlinear dimensionality reduction by maximum variance unfolding. In *Proceedings of the AAAI Conference on Artificial Intelligence*, volume 6, pp. 1683–1686, 2006a.

Weinberger, Kilian Q and Saul, Lawrence K. Unsupervised learning of image manifolds by semidefinite programming. *International journal of computer vision*, 70(1): 77–90, 2006b.

Weinberger, Kilian Q, Sha, Fei, and Saul, Lawrence K. Learning a kernel matrix for nonlinear dimensionality reduction. In *Proceedings of the twenty-first international conference on Machine learning*, pp. 106, 2004.

Weinberger, Kilian Q, Packer, Benjamin, and Saul, Lawrence K. Nonlinear dimensionality reduction by semidefinite programming and kernel matrix factorization. In *AISTATS*, 2005.

Weinberger, KQ and Saul, LK. Unsupervised learning of image manifolds by semidefinite programming. In *Proceedings of the 2004 IEEE Computer Society Conference on Computer Vision and Pattern Recognition*, volume 2. IEEE, 2004.

Weiss, Yair. Segmentation using eigenvectors: a unifying view. In *Proceedings of the seventh IEEE international conference on computer vision*, volume 2, pp. 975–982. IEEE, 1999.

Williams, Christopher and Seeger, Matthias. The effect of the input density distribution on kernel-based classifiers. In *Proceedings of the 17th international conference on machine learning*, 2000.

Yan, Shuicheng, Xu, Dong, Zhang, Benyu, and Zhang, Hong-Jiang. Graph embedding: A general framework for dimensionality reduction. In *2005 IEEE Computer Society Conference on Computer Vision and Pattern Recognition (CVPR'05)*, volume 2, pp. 830–837. IEEE, 2005.

Yan, Shuicheng, Xu, Dong, Zhang, Benyu, Zhang, Hong-Jiang, Yang, Qiang, and Lin, Stephen. Graph embedding and extensions: A general framework for dimensionality reduction. *IEEE transactions on pattern analysis and machine intelligence*, 29(1):40–51, 2006.

Zhang, Benyu, Yan, Jun, Liu, Ning, Cheng, Qiansheng, Chen, Zheng, and Ma, Wei-Ying. Supervised semidefinite embedding for image manifolds. In *2005 IEEE International Conference on Multimedia and Expo*, pp. 4–pp. IEEE, 2005.